

January 2012

Investigation of Various Surface Acoustic Wave Design Configurations for Improved Sensitivity

Greeshma Manohar

University of South Florida, greeshma@mail.usf.edu

Follow this and additional works at: <http://scholarcommons.usf.edu/etd>

 Part of the [Engineering Commons](#)

Scholar Commons Citation

Manohar, Greeshma, "Investigation of Various Surface Acoustic Wave Design Configurations for Improved Sensitivity" (2012).
Graduate Theses and Dissertations.
<http://scholarcommons.usf.edu/etd/4365>

This Thesis is brought to you for free and open access by the Graduate School at Scholar Commons. It has been accepted for inclusion in Graduate Theses and Dissertations by an authorized administrator of Scholar Commons. For more information, please contact scholarcommons@usf.edu.

Investigation of Various Surface Acoustic Wave Design Configurations for Improved
Sensitivity

by

Greeshma Manohar

A thesis submitted in partial fulfillment
of the requirements for the degree of
Master of Science in Mechanical Engineering
Department of Mechanical Engineering
College of Engineering
University of South Florida

Major Professor: Rasim Guldiken, Ph.D.
Nathan Crane, Ph.D
Muhammad Rahman, Ph.D.

Date of Approval:
October 29, 2012

Keywords: Inter Digital Transducer, Waveguide, Love Wave Sensor, Surface Transverse
Wave, Network Analyzer, Frequency Shift

Copyright © 2012, Greeshma Manohar

Dedication

I would dedicate this to my parents Manohar Hosmath and Geethamala N.M without them none of these would have been possible. I love you all and thank you so much for being with me all the time.

Acknowledgments

I would like to thank Dr. Rasim Guldiken, for his encouragement, supervision and support that made this thesis possible. He has been a wonderful mentor throughout my study and personal life in USF. I would also like to thank Onursal Onen for his direction and time for helping me throughout this work. I would like to show my gratitude to Dr. Muhammad Rahman and Dr. Nathan Crane for their valuable advice and time. I am very glad to have them in my committee. Finally I would like to thank Nanotechnology Research and Education Center for training me on all the instruments that I needed to make this thesis successful.

Table of Contents

List of Tables	iv
List of Figures	v
Abstract	vii
1. Introduction.....	1
1.1 Motivation and Objectives	1
1.2 Thesis Organization	2
2. Acoustic Wave Sensors	4
2.1 Sensors	4
2.2 Acoustic Wave Generation Principle.....	5
2.3 Acoustic Wave Modes	6
2.3.1 Bulk Acoustic Wave	6
2.3.1.1 Thickness Shear Mode (TSM).....	7
2.3.1.2 Shear Horizontal Acoustic Plate Mode (SH-APM).....	8
2.3.2 Surface Acoustic Wave (SAW)	9
2.3.2.1 Rayleigh Wave.....	10
2.3.2.2 Shear Horizontal Surface Acoustic Wave (SH-SAW).....	10
2.3.2.3 Love Wave (LW)	11
2.3.2.4 Surface Transverse Wave (STW)	12
2.3.2.5 Surface Skimming Bulk Wave (SSBW).....	13
2.4 Common Terminology and Methods	14
2.4.1 Piezoelectric Effect	15
2.4.2 Substrate Selection.....	16
2.4.3 Inter Digital Transducer (IDT).....	17
2.4.4 Metallization	20
2.4.5 Photo Resist and its Function.....	20
2.4.6 Developer and its Function	21
2.4.7 Etching	21
3. Design, Fabrication and Testing	23
3.1 Sensor Design	23
3.2 Fabrication	24
3.2.1 Wafer Preparation	24
3.2.2 Sputter Coating	25

3.2.3	Alpha-Step Profilometer	27
3.2.4	Spin Coating.....	27
3.2.5	Photo Lithography	30
3.2.6	Developing.....	33
3.2.7	Wet Etching	35
3.2.8	Waveguide Deposition.....	36
	3.2.8.1 Spin Coating (SU8-2035)	37
	3.2.8.2 Plasma Enhanced Chemical Vapor Deposition (PECVD).....	37
3.2.9	Dicing Saw	39
3.3	Sensor Preparation	41
3.4	Testing Instruments.....	42
	3.4.1 Network Analyzer.....	42
	3.4.2 Multi-meter	43
	3.4.3 Convection Oven	43
3.5	Experimental Setup.....	44
3.6	Data Analysis	47
4.	Results and Discussion	49
	4.1 Comparison of In-house Sputtered and Outside Sputtered Sensors	49
	4.1.1 Comparison of Bi-directional Electrode Sensors.....	49
	4.1.2 Comparison of Split Electrode Sensors	53
	4.1.3 Comparison of STW Sensors.....	56
	4.1.4 Comparison of SPUDT Sensors	59
	4.1.5 Summary.....	62
	4.2 Comparison Love Wave Sensors with SU8 and SiO ₂ as Waveguide.....	63
	4.2.1 Comparison of Bi-directional Electrode Love Wave Sensors	64
	4.2.2 Comparison of Split Electrode Love Wave Sensors	67
	4.2.3 Comparison of STW Love Wave Sensors	70
	4.2.4 Comparison of SPUDT Love Wave Sensors	73
	4.2.5 Summary	76
5.	Conclusion and Future Work	78
	5.1 Conclusion	78
	5.2 Future Work.....	80
	References.....	81
	Appendices.....	87
	Appendix A: Fabrication Recipes.....	88
	Appendix B: Instrumentation.....	91
	Appendix C: Copyright Permissions	96
	C.1: Permission for Figure 2, Figure 3, Figure 4 (a) and Figure 5	96
	C.2: Permission for Table 1	97
	C.3: Permission for Figure 12, Figure 13 and Figure 14	98

C.4: Permission for Figure 9 (b)	100
C.5: Permission for Figure 11, Figure 15 and Figure 20	100

List of Tables

Table 1: Substrates used for acoustic wave generation	16
Table 2: Comparison of in-house and outside sputtered sensors	62
Table 3: Comparison of SU8 and SiO ₂ coated sensors.....	76
Table A1: Design parameters.....	88
Table A2: Sputtering condition.....	89
Table A3: Recipe for spin coating	89
Table A4: PECVD recipe for growing SiO ₂	90
Table A5: Dicing saw recipe.....	90
Table B1: Instruments used for this study	91

List of Figures

Figure 1: Sensor system	4
Figure 2: Typical acoustic wave device.....	6
Figure 3: Typical TSM resonator.....	7
Figure 4: (a) SH-APM device and (b) SH-APM working principle.....	8
Figure 5: Surface acoustic wave device.....	9
Figure 6: Rayleigh wave propagation	10
Figure 7: SH-SAW device	11
Figure 8: (a) Love wave device and (b) Propagation.....	12
Figure 9: (a) STW device and (b) Propagation	13
Figure 10: (a) SSBW with wave propagation pattern and (b) Propagation into substrate	14
Figure 11: Transformation of mechanical energy to electrical energy	15
Figure 12: Bi-directional electrode	19
Figure 13: Split electrode.....	19
Figure 14: SPUDT electrode.....	19
Figure 15: Schematic view of plasma etching process	22
Figure 16: Typical DC sputtering principle	25
Figure 17: Spin coat process	28
Figure 18: (a) Contact printing, (b) Proximity printing and (c) Projection printing.....	31

Figure 19: Difference between positive and negative resist	33
Figure 20: Typical PECVD process.....	38
Figure 21: Sensor connection.....	41
Figure 22: Basic working principle of network analyzer.....	43
Figure 23: Convection oven principle.....	44
Figure 24: Experimental setup.....	45
Figure 25 Sensor response at different temperature	48
Figure 26: Frequency shift for in-house sputtered bi-directional IDT sensor	51
Figure 27: Frequency shift for outside sputtered bi-directional IDT sensor.....	52
Figure 28: Frequency shift for in-house sputtered split electrode sensor	54
Figure 29: Frequency shift for outside sputtered split electrode sensor	55
Figure 30: Frequency shift for in-house sputtered STW sensor	57
Figure 31: Frequency shift for outside sputtered STW sensor	58
Figure 32: Frequency shift for in-house sputtered SPUDT sensor.....	60
Figure 33: Frequency shift for outside sputtered SPUDT sensor	61
Figure 34: Frequency shift for SU8 coated bi-directional electrode sensor	65
Figure 35: Frequency shift for SiO ₂ coated bi-directional electrode sensor.....	66
Figure 36: Frequency shift for SU8 coated split electrode sensor	68
Figure 37: Frequency shift for SiO ₂ coated split electrode sensor.....	69
Figure 38: Frequency shift for SU8 coated STW sensor	71
Figure 39: Frequency shift for SiO ₂ coated STW sensor.....	72
Figure 40: Frequency shift for SU8 coated SPUDT sensor.....	74
Figure 41: Frequency shift for SiO ₂ coated SPUDT sensor	65

Abstract

Surface acoustic wave sensors have been a focus of active research for many years. Its ability to respond for surface perturbation is a basic principle for its sensing capability. Sensitivity to surface perturbation changes with every inter-digital transducer (IDT) design parameters, substrate selection, metallization choice and technique, delay line length and working environment.

In this thesis, surface acoustic wave (SAW) sensors are designed and characterized to improve sensitivity and reduce loss. To quantify the improvements with a specific design configuration, the sensors are employed to measure temperature. Four SAW sensors design configurations, namely bi-directional, split electrode, single phase unidirectional transducer (SPUDT) and metal grating on delay line (shear transvers wave sensors) are designed and then fabricated in Nanotechnology Research and Education Center (NREC) facility using traditional MEMS fabrication processes. Additionally, sensors are then coated with guiding layer SU8-2035 of 40 μ m using spin coating and SiO₂ of 6 μ m using plasma enhanced chemical vapor deposition (PECVD) process. Sensors are later diced and tested for every 5 $^{\circ}$ C increment using network analyzer for temperature ranging from 30 $^{\circ}$ C \pm 0.5 $^{\circ}$ C to 80 $^{\circ}$ C \pm 0.5 $^{\circ}$ C. Data acquired from network analyzer is analyzed using plot of logarithmic magnitude, phase and frequency shift.

Furthermore, to investigate the effect of metallization technique on the sensor performance, sensors are also fabricated on substrates that were metallized at a commercial MEMS foundry. All in-house and outside sputtered sensor configurations are compared to investigate quality of sputtered metal on wafer. One with better quality sputtered metal is chosen for further study. Later sensors coated with SU8 and SiO₂ as guiding layer are compared to investigate effect of each waveguide on sensors and determine which waveguide offers better performance.

The results showed that company sputtered sensors have higher sensitivity compared to in-house sputtered wafers. Furthermore after comparing SU8 and SiO₂ coated sensors in the same instrumental and environmental condition, it was observed that SU8 coated di-directional and single phase unidirectional transducer (SPUDT) sensors showed best response.

1. Introduction

Surface acoustic wave (SAW) sensors are known for ruggedness, reliability, low cost, and simplistic design [1]. Because of these characteristics SAW sensors have been a focus of active research in many fields including but not limited to medicine, automobile, material properties and measuring physical parameters [1]. Commercially available SAW sensors are mainly employed as filters for communication and various electronic devices. In this thesis SAW sensors with different designs configurations and guiding layers are investigated at varying temperature for potentially higher sensitivity and lower loss operation [2].

1.1 Motivation and Objectives

This work is motivated due to desirability of more sustainable and inexpensive temperature sensor for its use in medical devices, automobiles, and other application [1].

Desirable characteristics of acoustic wave sensors are; faster response, high sensitivity, low cost, portability and miniature size [2]. This thesis focuses on improving sensitivity by decreasing loss and signal reflection. Main core of this research is to design sensors and employ different waveguide materials to enhance the sensitivity.

The main objectives for this research are:

1. Investigating sensors with different inter-digital transducer design configurations and comparing their performance at different temperatures.
2. Investigating sensors with different wave guide material and analyzing them at different temperatures.

1.2 Thesis Organization

This thesis is organized in such a way that, chapter 2 gives all the basic terminology used in acoustic sensors. This helps for better understanding about the later part of research. Each chapter details are given below:

1. Chapter 2: Starts with very basic sensors principles, with more detail in acoustic wave generation and different modes of it. Later part of this chapter briefs about basic terminology required for designing and fabricating sensors.
2. Chapter 3: This section discusses new sensor design and fabrication. Here brief introduction about instruments used for fabrication are reviewed, which aids in better understanding for readers. This section also includes recipes followed to fabricate each sensor. Additionally, sensor characterization at different temperature is discussed with all the circuit connections and experimental setup.
3. Chapter 4: Here tested sensors are analyzed and compared for different sensors with different wave guides.

4. Chapter 5: This chapter summarizes the entire research and discusses potential future work with the current research.

2. Acoustic Wave Sensors

2.1 Sensors

Sensors are used in almost every field these days ranging from very basic home appliances, advanced medical devices, automotive industry to space vehicles. Investigation of new types of sensors is required to address the needs of the developing technology. Hence sensors have become emerging technology and currently being investigated in wide-variety of technological areas [1].

Sensors convert one form of energy to another. This is accomplished by detecting the measurand, converting it to a readable signal which carries information which is later converted to useful form [2]. Sensor system has two components transducer and signal processor as shown in Figure 1.



Figure 1 Sensor system

All the components in a sensor system play vital role. Measurand for the sensor depends on its application. For this study, temperature is chosen to be the quantifiable measurand. This is sensed using a component called transducer. Depending on the type of measurand transducer is selected, but every transducer works essentially the similar way. For this study, piezoelectric transducers are investigated, as acoustic waves can be more efficiently generated from piezoelectric transducers. Finally signal processor, which is chosen based on type of output signal needed. It can range from a basic electrical circuit to complex instruments [2].

2.2 Acoustic Wave Generation Principle

Acoustic wave devices have been in use for the past 60 years [3]. In the past two decades, acoustic-wave devices have gained enormous interest for sensor applications. Acoustic wave devices are attractive for use in sensors due to the fact that wave velocity and damping are sensitive to outside parameters [4].

Typical acoustic micro device consists of a piezoelectric material with one or more metal inter-digital transducers on its surface. These transducers launch wave combined with a confinement structure to produce a standing wave in the material at ultrasonic frequencies. The transducer metal is usually selected for either chemical inertness or for its acoustic match to the piezoelectric material [5]. Crystal orientation, thickness of the piezoelectric material and the geometry of the metal transducers determine the type of acoustic wave generated [5, 6].

2.3 Acoustic Wave Modes

Distinction between sensor types can be made according to velocities and displacement direction in different devices. Depending on material type and boundary conditions different configurations are possible. The inter-digital transducers (IDT) produce electrical voltage necessary for acoustic wave generation. The wave generated propagates through or on the substrate and is converted back to electric field carrying data at the other IDT [6]. Figure 2 shows the typical configuration of an acoustic wave device.

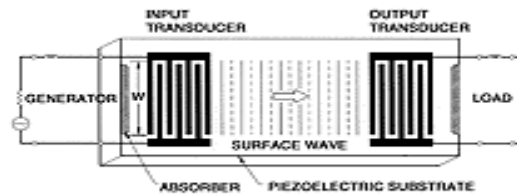


Figure 2 Typical acoustic wave device [6]

2.3.1 Bulk Acoustic Wave

If the wave propagates through the substrate, the wave is called a bulk wave [5]. In the bulk of a substrate, two types of bulk acoustic waves (BAW) can propagate. They are the longitudinal waves, also called compressional/extensional waves, and the transverse waves, also called shear waves, where particle motion is parallel and perpendicular to the direction of wave propagation respectively [7,8]. Some of the

popular bulk acoustic wave (BAW) devices are the thickness shear mode (TSM) resonator and the shear-horizontal acoustic plate mode (SH-APM) sensors [6].

2.3.1.1 Thickness Shear Mode (TSM)

The TSM which is also as quartz crystal microbalance (QCM) is one of the oldest and simplest configuration of acoustic wave device [6]. In TSM device crystal resonates when electromechanical waves are created, hence this device is commonly used as resonator. TSM resonator can detect and measure liquid properties, making it a good candidate for a biosensor [9]. TSM features simple fabrication, ability to withstand harsh environments and temperature stability. The application of electric voltage into IDTs would lead to shear deformation in the crystal. The displacement is throughout the thickness of the plate and maximum at the surfaces making device sensitive to surface interaction. Only disadvantage of TSM device is, it has low mass sensitivity [10, 11]. A typical TSM is shown in Figure 3.

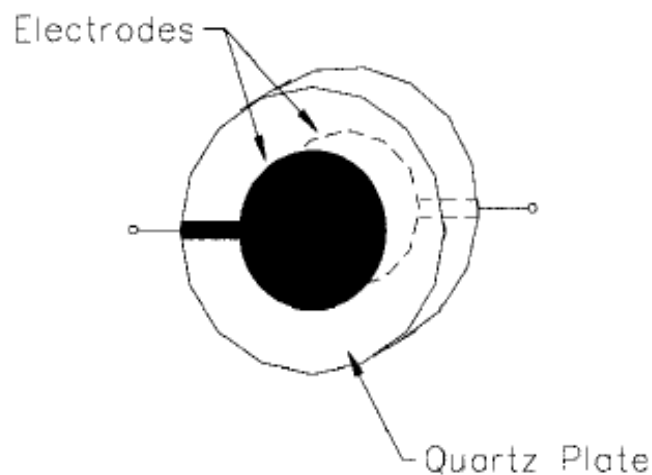


Figure 3 Typical TSM resonator [6]

2.3.1.2 Shear Horizontal Acoustic Plate Mode (SH-APM)

SH-APM sensors use a thin piezoelectric substrate or plate that serves as an acoustic waveguide, confining the energy between the upper and lower surfaces of the plate [6]. As a result in SH-APM device both surfaces undergo displacement on applying voltage and hence both surfaces can be used for detection. This is an important advantage for SH-APM as one side containing IDTs can be isolated and protected from conducting fluids or gases and the other surface can be used for sensitivity [12]. Sensitivity of SH-APM device depends on thickness of substrate, as the device gets thinner sensitivity to mass loading and other perturbation increases. [13]. Hence fabrication is a challenging and expensive. Figure 4 shows wave generation principle and SH-APM device.

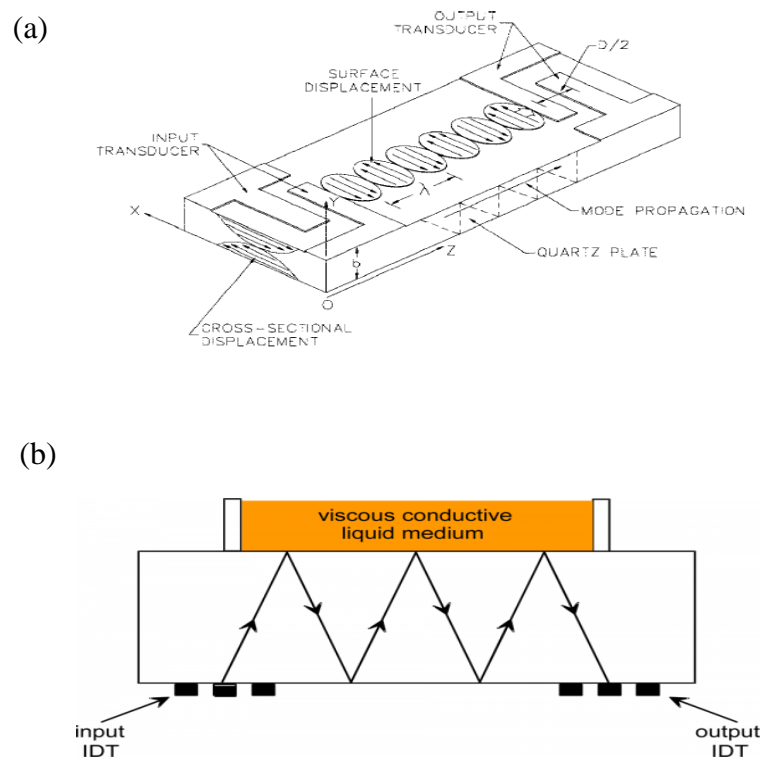


Figure 4 (a) SH-APM device [6] and (b) SH-APM working principle [12]

2.3.2 Surface Acoustic Wave (SAW)

Surface acoustic waves were discovered in 1885 by Lord Rayleigh [14]. The operation of the SAW device is based on acoustic wave propagation near the surface of a piezoelectric solid. This implies that the wave can be trapped or otherwise modified while propagating [15]. The displacements decay exponentially away from the surface, so that the most of the wave energy is confined within a depth of substrate [16]. SAW device typically has two IDTs on a piezoelectric substrate. The input IDT launches the wave and the output IDT receives the propagating waves [6]. Depending on the wave energy confinement SAW is classified into different modes. Figure 5 shows the typical SAW device with wave generation in Z direction.

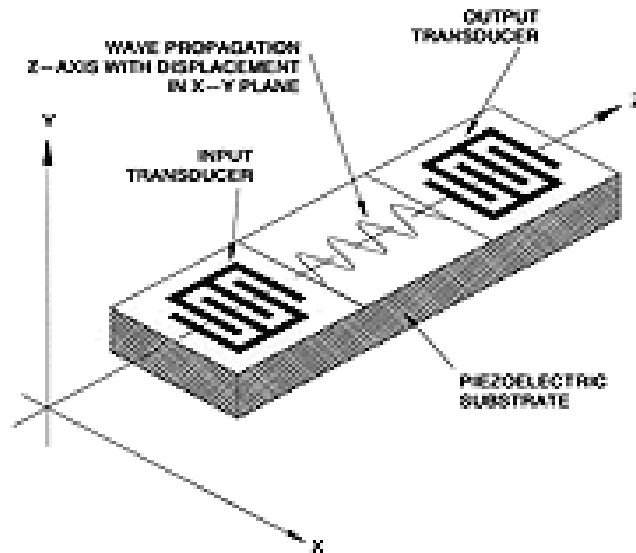


Figure 5 Surface acoustic wave device [6]

2.3.2.1 Rayleigh Wave

The elastic Rayleigh wave has both a surface-normal component and a surface-parallel component with respect to the direction of propagation. The Rayleigh wave has two particle displacement components. Surface particles here move in elliptical paths having a surface-normal and a surface-parallel component [17]. The wave velocity is determined by the substrate material and the crystal orientation. The energy of the SAW is confined to a zone close to the surface and is only few wavelengths thick [18]. Figure 6 shows Rayleigh wave propagation, it can be seen that displacement is elliptic along vertical plane for Rayleigh wave along the wave direction.

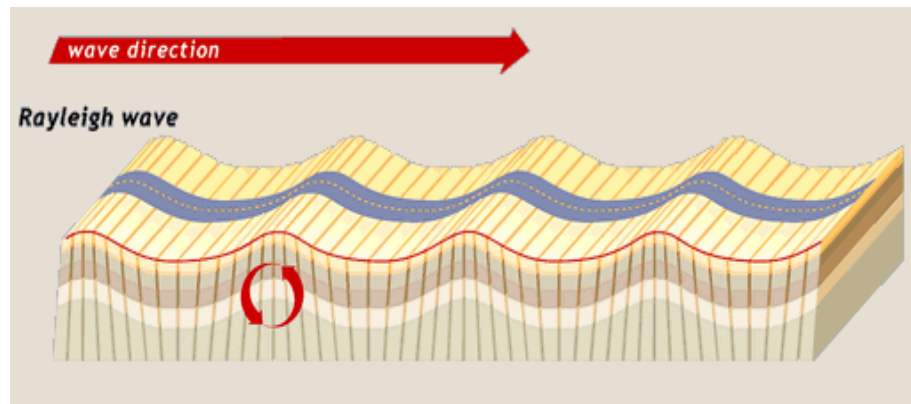


Figure 6 Rayleigh wave propagation [19]

2.3.2.2 Shear Horizontal Surface Acoustic Wave (SH-SAW)

This was the first sensor which used leaky waves, where the wave is only partially confined to the surface. This wave extends several wavelengths into the device and therefore has a good sensitivity to changes at the device surface. For SH-SAW by using proper orientation of substrate, the wave mode can be changed from a vertical shear wave

to a shear-horizontal wave [20]. This reduces loss and confines wave to surface of substrate, allowing the SH-SAW sensor to operate efficiently in both liquid and gas media [6]. Figure 7 shows SH-SAW propagation along the substrate.

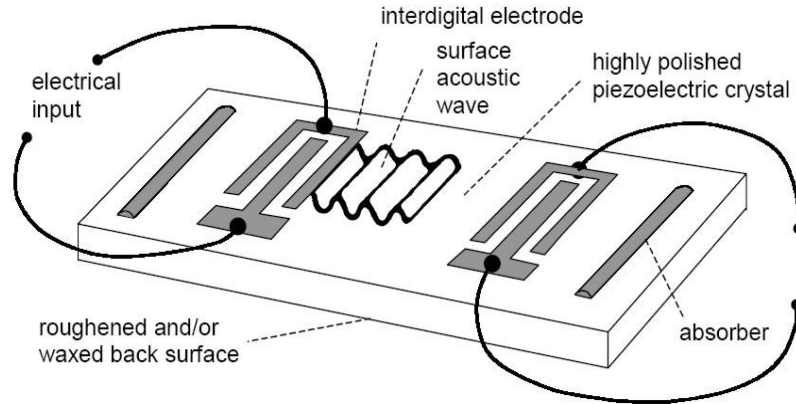


Figure 7 SH-SAW device [21]

2.3.2.3 Love Wave (LW)

The wave confinement in this case obtained by depositing a layer of a material with low acoustic wave velocity over a substrate with infinite thickness, where two IDTs are realized. Such an added overlayer, typically of silicon dioxide or polymethylmethacrylate (PMMA), works as a waveguide and keeps most of the vibration energy localized close to the surface, regardless of the plate thickness [22]. As these waves are transverse they bring only shear stresses into action. Because of its active responsive to surface perturbation and high mass sensitivity, Love wave sensors are typically used for liquid application [23]. Figure 8 showing the racking motion along vertical and horizontal plane.

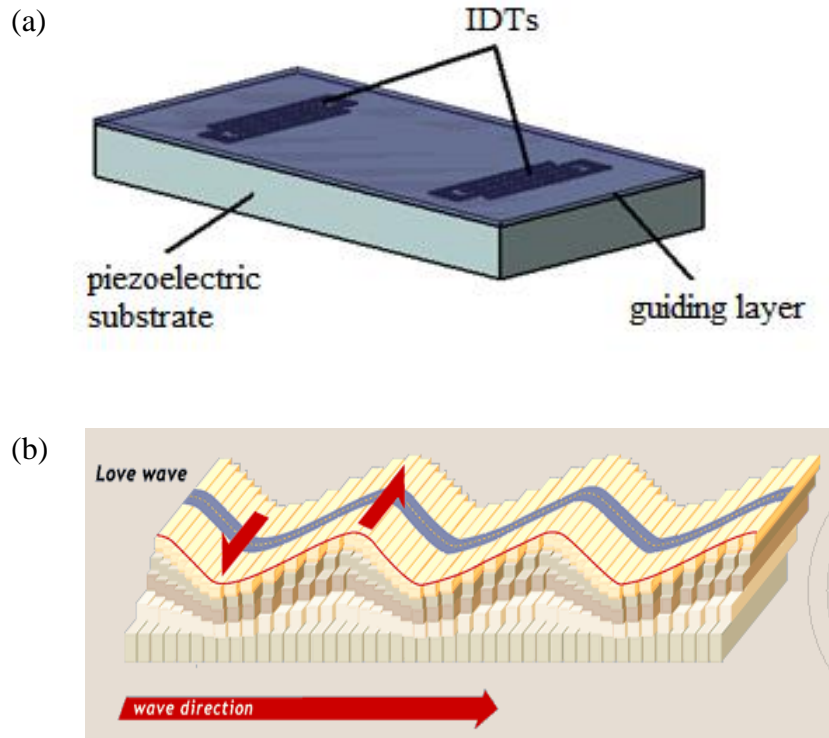


Figure 8 (a) Love wave device [12] and (b) Propagation [19]

2.3.2.4 Surface Transverse Wave (STW)

Surface transverse wave (STW) sensors are devices in which shear vibrations are confined to surface on the face where the IDTs are placed [6]. This wave confinement is obtained by inserting a metallic grating on the delay line between the IDTs that introduces a periodic perturbation in the wave path and lowers the wave velocity at the surface [25]. Since the vibration energy density is concentrated on the metal grating near the surface, the device is very responsive to surface perturbations and, in particular, it provides a high mass sensitivity. This allows it to be used for liquid sensing application [26]. Figure 9 shows waves confined to the surface using metal grating.

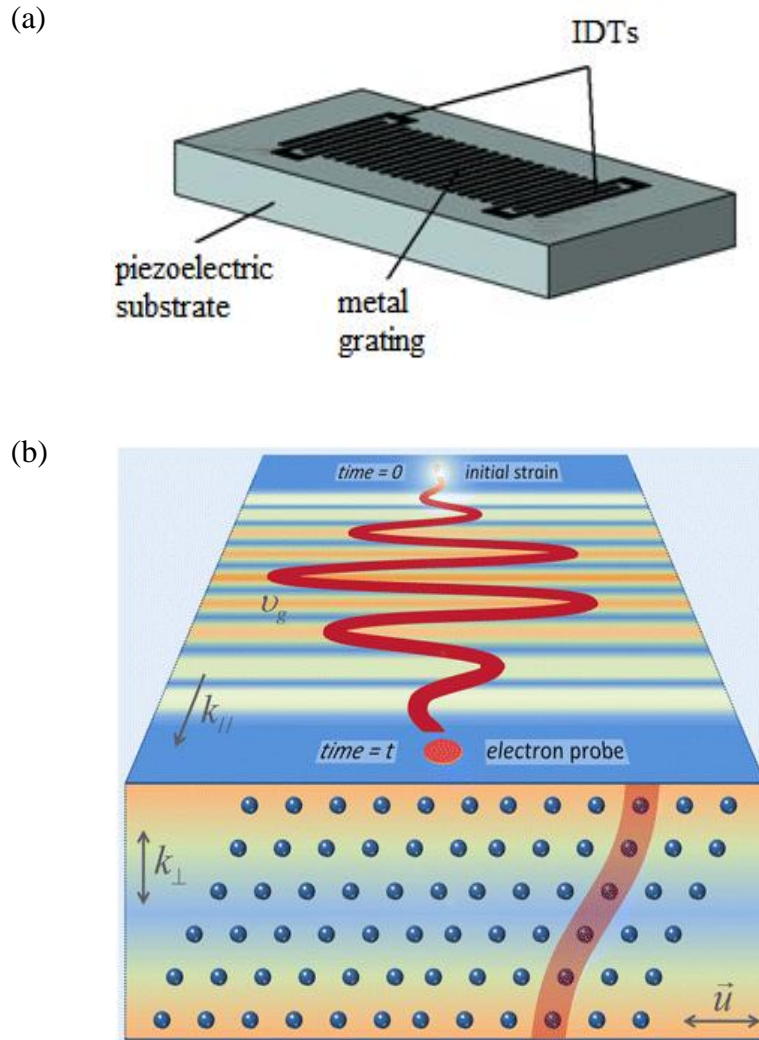


Figure 9 (a) STW device [12] and (b) Propagation [27]

2.3.2.5 Surface Skimming Bulk Wave (SSBW)

Surface skimming bulk waves are horizontally polarized bulk shear waves which travel just beneath surface of the substrate. SSBW initially discredited due to loss in signal strength from radiation into the bulk of the substrate [28]. But by depositing a thin film or a grating pattern on the propagation path the energy of these waves can be confined close to the surface and surface transverse waves can be realized. Delay line

devices based on SSBW mode launch transverse bulk waves with propagation vector normal to x -axis and parallel to surface (surface skimming). The particle displacements in these waves is shear horizontal therefore no significant attenuation occurs when immersed in liquid medium [29]. The advantage of SSBW device is that, it is less sensitive to surface contamination. This should ease the long term ageing problem in oscillators, and generally ease fabrication and packaging problems [30].

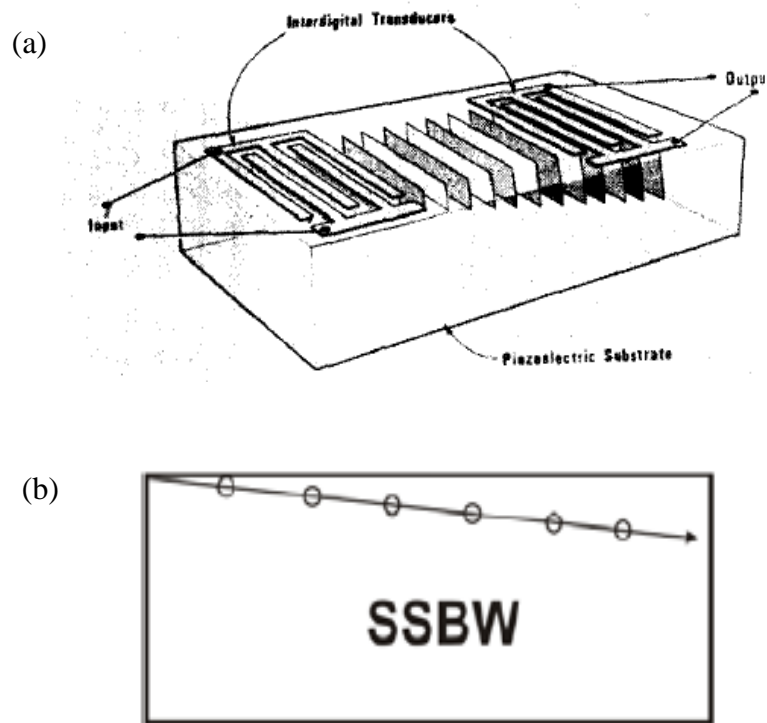


Figure 10 (a) SSBW device with wave propagation pattern [28] and (b) Propagation into substrate [12]

2.4 Common Terminology and Methods

Some very common terminologies and methods that are used in Acoustic wave sensor industry are discussed in this section.

2.4.1 Piezoelectric Effect

Piezoelectric crystals play a very important role in the communications and electronics industry. The piezoelectric effect can be demonstrated by applying either a compressive or tensile stress to a piezoelectric crystal. This effect results in electrical charge appearing on the surface of the electrodes. When the force is removed, the strain within the crystal lattice is released causing charge to flow, thus reestablishing a zero potential difference between the electrodes [5]. If a stress alternating between the tensile and compressive forces is applied to opposite crystal faces, a sinusoidal piezoelectric voltage will appear across the electrodes. In this case, electrical energy is produced from mechanical energy. This can be reversed to get piezoelectric microactuators [32]. Figure 11 shows the principle of piezoelectric effect

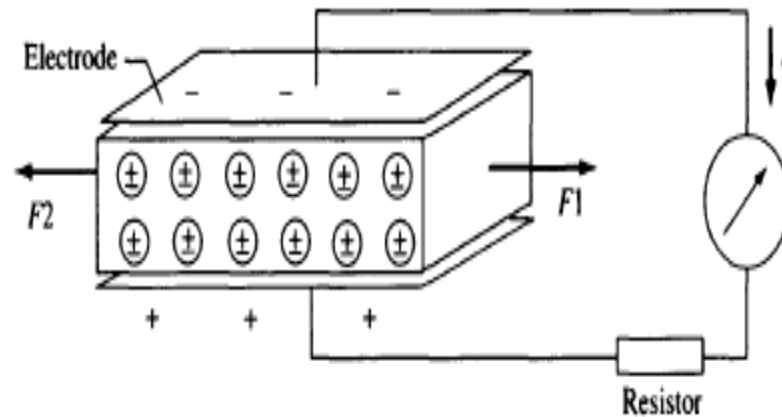


Figure 11 Transformation of mechanical energy to electrical energy [18]

2.4.2 Substrate Selection

Basic principle for acoustic wave generation is due to piezoelectric effect and this is achieved using piezoelectric substrates [1]. There are several piezoelectric substrate materials that may be used for acoustic wave device. The most popular piezoelectric substrates are quartz (SiO_2), lithium tantalate (LiTaO_3), and lithium niobate (LiNbO_3). Each material has specific advantages and disadvantages and is chosen considering its application, cost, temperature dependence, attenuation, and propagation velocity [6]. Quartz is one of the commonly used substrate material because of its low cost and its property of selecting the temperature dependency of material by choosing proper orientation of crystal cut [33]. Acoustic wave temperature sensor may be designed by maximizing this effect. This does not hold for LiNbO_3 or LiTaO_3 , where linear temperature dependence always exists for all material cuts and propagation directions [34]. Table 2.1 shows some popular substrates used for acoustic wave generation.

Table 1 Substrates used for acoustic wave generation [33]

Substrate	SAW Velocity v (m/s)	K^2 (%)	1st-Order TCD Mag. (ppm/°C)	Comments
ST-quartz:	3158	0.14	0	Up to 25 cm long, Ref. [26].
Y-Z LiNbO_3 :	3488	4.5	94	Up to 25 cm long
128°rotated-Y X LiNbO_3 :	3992	5.3	75	Up to 25 cm long
SiO_2 on 128°-Y X LiNbO_3 :	$\approx 3800?$	≈ 8.0	≈ 0	Large K^2 , Ref. [63]
$\text{Bi}_{12}\text{GeO}_{20}$:	1681	1.4	120	(110)-cut, $\langle 001 \rangle$ -propagation
GaAs:	<2841	<0.06	35	For (100)-cut with $\langle 110 \rangle$ propagation.
Rotated-Y cut Z'-prop. LiTaO_3 :	3254	0.72	35	Minimum diffraction cut, Ref. [53]
X-cut 112°				
Y-prop LiTaO_3 :	3288	0.6	18	Low bulk wave emission
X-Z $\text{Li}_2\text{B}_4\text{O}_7$:	3562	≈ 1	6.2	Can dissolve in water and acids, Ref. [55]
ZnO/AlN/Glass:	5840	4.3	21	Uses Sezawa mode of Rayleigh wave, Ref. [58].

2.4.3 Inter Digital Transducer (IDT)

The IDT is a very important part of SAW technology. Its function is to convert electrical energy into mechanical energy, and vice versa, for generating and detecting the SAW. The structure of the IDT is typically fabricated onto the thin film that has been deposited onto the surface of a piezoelectric substrate using lithography steps [18]. An IDT excites an acoustic wave in the piezoelectric substrate when a voltage signal is applied to it. This varying voltage results in varying deformation of the piezoelectric substrate leading to generation of an acoustic wave. The wavelength of the wave excited by the IDT is equal to the periodicity of the IDT pattern [35].

Operation frequency, bandwidth, and electrical impedance depend on parameters of IDT design including electrode width, spacing, width of IDT, delay path length and number of finger pairs [36].

To design SAW device with given resonant frequency f_o and fractional bandwidth $B\alpha f_o/\lambda$ (Measured null to null from either side of resonant frequency). Following equations are used.

Acoustic wavelength can be obtained using

$$\lambda = \frac{v_o}{f_o} \quad (1)$$

where v_o is the SAW velocity for the substrate selected and f_o is the resonance frequency.

Number of finger pairs, N needed to achieve this fractional bandwidth

$$N = 2/B \quad (2)$$

IDT behaves as a capacitive system. To determine the total capacitance, C_t of an IDT equation 3 is used.

$$C_t = 1/ (2\pi f_o Z) \quad (3)$$

For best response, impedance Z of IDT should match with impedance of the measurement system (around 50 ohms).

Aperture, W (overlapped fingers for IDT) is given by:

$$W = C_t/ C_o N \quad (4)$$

To enhance the sensor performance and stability, insertion loss and unwanted spurious effects must be reduced. These reductions can be achieved by using a piezoelectric substrate with a high electro-mechanical coupling coefficient and controlling a few parameters, such as the IDT type, IDT length, aperture width and delay line length. Among these, IDT type is the most important parameter for realizing low insertion loss and improving device stability. Some IDT designs are discussed below [37].

Bi-directional electrode shown in Figure 12 the bidirectional IDT with uniform finger spacing consists of a grating structure with intervals of $\lambda/4$.

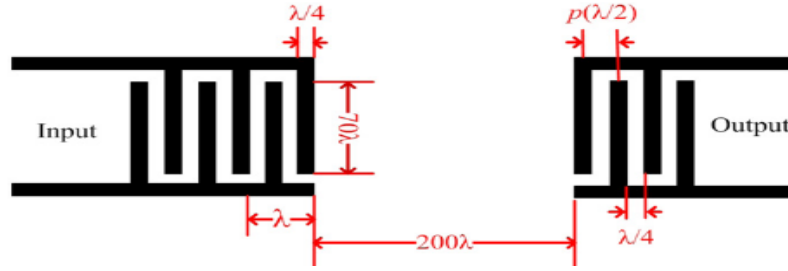


Figure 12 Bi-directional electrode [37]

The split IDT (Figure.13) is composed of a grating structure with intervals of $\lambda/8$ with a center to center distance of $\lambda/4$. Typical IDT structure has the disadvantage of higher insertion loss and lower frequency stability than the split IDT.

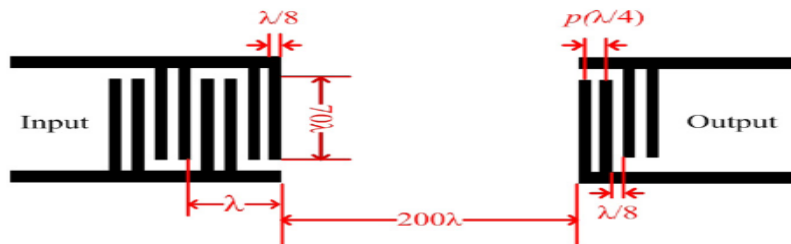


Figure 13 Split electrode [37]

In Single phase unidirectional transducer (SPUDT – Figure 14) finger width of $\lambda/4$ and $\lambda/8$ and interval spacing of $\lambda/8$ and $3\lambda/16$ is considered. Reason for lowered insertion loss is due to decreased Bragg's reflection.

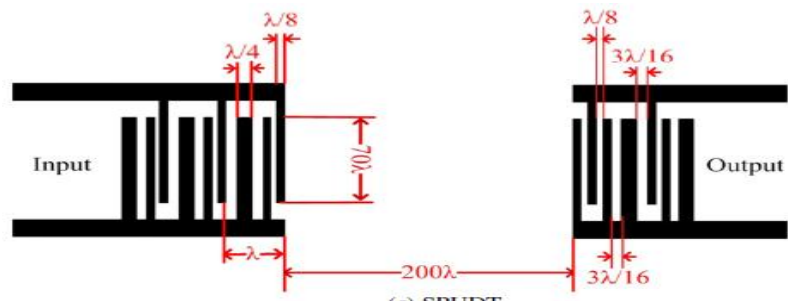


Figure 14 SPUDT electrode [37]

2.4.4 Metallization

Metallization is necessary to get adequate electrical conductivity and for wave excitation. Based on the need, metal type is decided. Commonly used metals are gold, chromium and aluminum. Metallization can be achieved in different ways. For example sputtering, e-beam evaporator, chemical vapor deposition. Type of metallization process chosen depends on desired quality and time. In the later part of lithography metal coated, will be etched to get desired sensors [36].

2.4.5 Photo Resist and its Function

Photo resist is organic compound whose chemical properties change when exposed to ultraviolet rays due to breaking of chemical bonds. Resist is spun on the wafer by spin coating process. Thickness of resist is varied by varying spin speed and time [36].

Two basic parameters that describe resist properties are contrast and critical modulation transfer function (CMTF). Contrast is the ability of resist to distinguish between light and dark portion. So resist with high contrast gives sharp lines and edges. CMTF is the dark v/s light intensities in the aerial image produced by the exposure system which on combination with contrast gives the scale of resolution or sharpness. Also reflection from surface exposing decreases resolution [38, 39].

There are 2 types of resist positive and negative. UV light exposure renders positive resist more soluble in developer but negative resist renders thin soluble in developer [18].

2.4.6 Developer and its Function

Photoresist developers are used in lithography process to create patterned image projected onto the photoresist of substrate. Developer is the chemical used after expose to selectively dissolve resist as a function its chemical composition. Ideally, we want a large difference in developer solubility between exposed and unexposed resist. The developer can be aqueous or solvent [38, 18].

Developers are segmented by their chemical type (organic or inorganic) and their solubility (i.e. strength of developer) [40].

2.4.7 Etching

Etching is one of the important procedures in micro-fabrication process. Etching is used in material processing for detailing patterns after developing, removing surface damage and contamination, and fabricating structures onto wafer surface. Etching of material is due to chemical reaction between the etchant and the material to be etched. Etching can be wet or dry. If the etching process use chemical solution as etchant it is called wet etching and if it use glow discharge (plasma) as etchant process is called dry etching [41, 18].

Basically wet etching is characterized by 4 parameters. Etch rate, material etching, Thickness to be etched and etch selectivity.

The basic concept of plasma or dry etching is, using glow discharge (i.e. plasma) that generates chemically reactive species on collision with an inert gas. The etching gas

is chosen depending on its reaction with material to be etched and its ability to produce reaction product that is volatile in nature. The etch product from the material etched is finally removed using vacuum system [18, 41]. Figure 15 shows schematic view of plasma etching process.

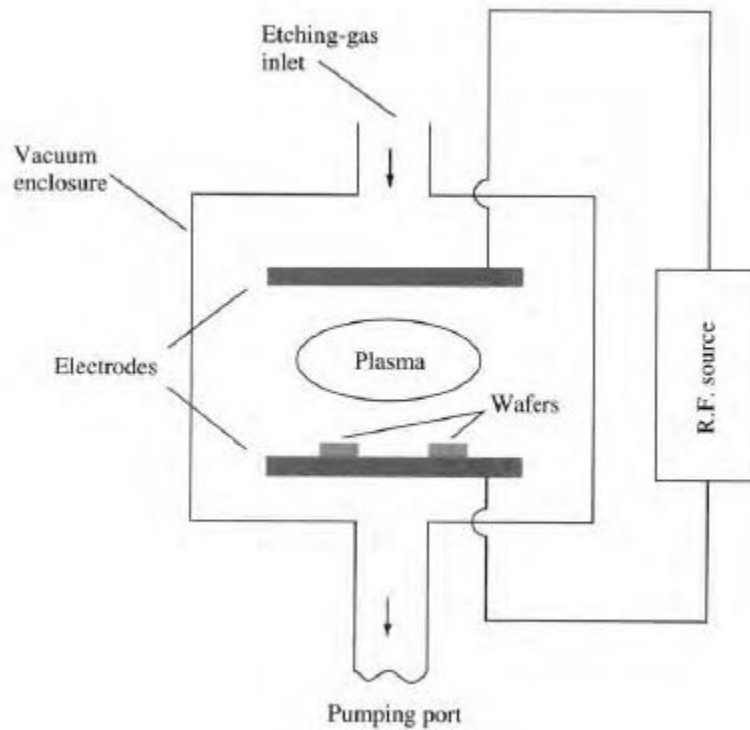


Figure 15 Schematic view of plasma etching process [18]

3. Design, Fabrication and Testing

3.1 Sensor Design

The design procedure for acoustic sensors is device and application specific. Issues such as acoustic mode selection and sensitivity, substrate selection, type of metallization and transducer geometry all need to be considered when investigating acoustic sensor designs. The final operational environment is also an important influence in the design procedure [42].

For this study 90° ST-Quartz (stable temperature quartz) with thickness of 0.5mm and diameter 89mm (3 inch) is used as substrate. Chrome with thickness of 1000°A is sputtered on the wafer. Then desired pattern is obtained on the substrate by photo lithography.

Before lithography, mask has to be judiciously designed with desired pattern on it. This can be accomplished using commercial design software, such as AutoCAD, LTspice, L-edit and more. For this work L-edit layout editor by Tanner research Inc. version 7.1.2 is used because of its large collection of transducer metals and simple and user friendly operation [43].

Using L-edit layout editor with chrome chosen as metal layer, a mask is designed with desired IDT geometry, bonding pads geometry and delay path length for a 3 inch wafer. Design parameters used are given in Table A1 of Appendix. Designed mask is then outsourced to company (Image Technology Precision Photomasks, Palo Alto, CA) for production.

3.2 Fabrication

Quality and sensitivity of the sensor not only depend on its design but also depend on instruments and methods used for fabrication. This section discusses about fabrication instruments and methods used for this study.

3.2.1 Wafer Preparation

Effective cleaning of wafer is a vital first fabrication step, which is essential for successful fabrication of IDT microsensors. In order to obtain good adhesion and a uniform coating of the metallic film used to make the IDT, a thorough cleaning of the wafer surface is essential. The cleaning of the wafers should be performed in a clean room to allow the safe and fast removal of any possible harmful fumes produced during the cleaning process [18, 41].

The wafers are initially cleaned by rinsing it with acetone followed by methanol rinse and finally with deionized water. This will remove surface contaminants, such as dust, grease and other particles. Further cleaning is then undertaken for the removal of the more obstinate contaminants. Wafer is then placed in acetone bath and subjected to ultrasonic agitation at room temperature for 10 minutes using ultrasonic cleaner. Then it

is rinsed by deionized water and later dried using compressed nitrogen and stored in a clean container to use it for sputtering [44]. Appendix B shows ultrasonic cleaner used for this work.

3.2.2 Sputter Coating

Metal layer can be deposited on the substrate by different ways. For this work sputtering coating process is chosen for metallization. Basic principle of sputter coating is, glow discharge formed between a cathode and anode using a suitable inert gas (typically argon). Then the bombardment of the cathode target material with gas ions will erode target, this process is called sputtering. The resulting deposition of sputtered atoms will form an even coating on the surface of the specimen [45]. Figure 16 shows basic working principle of DC sputtering.

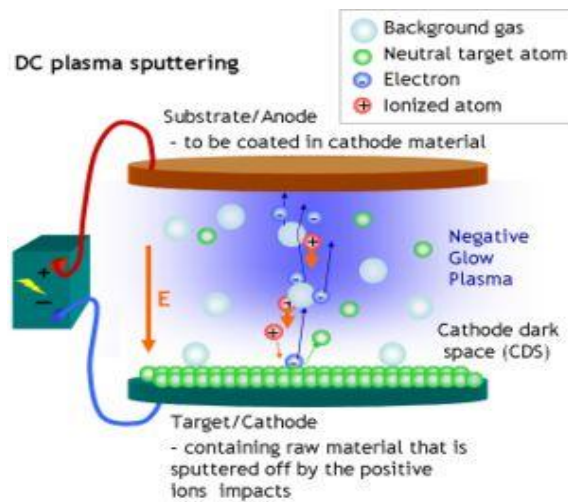


Figure 16 Typical DC sputtering principle [46]

For this study chrome is chosen as the transducer metal. Chrome is sputter coated on ST-quartz using CRC-100 sputter coater. Thickness of around 1000\AA is deposited on

a cleaned surface of an ST-quartz wafer. Appendix B shows CRC-100 sputter coater system used for this research.

Procedure followed for sputtering is as follows:

- Chrome target is installed to the system.
- Cleaned ST-quartz with coating surface facing upwards is placed inside chamber, note that chamber must be thoroughly cleaned before sputtering.
- Chamber is then closed and current type is switched to DC voltage.
- Argon gas to the chamber is turned on and allowed into the chamber to replace air.
- After the entire pre-start checkup, power to sputtering system is turned on.
- Rouging motor is turned on, once pressure in the chamber reaches below 100torr turbo motor is turned on, switching on turbo motor above 100torr will damage motor.
- Then wait till chamber reach 0.01torr, more the waiting time lesser the contaminants in the chamber and better the metal coating.
- After reaching 0.01torr power to the target is switched on. Sputtering is carried keeping system in constant voltage form. By setting voltage for known time desired thickness of metal can be achieved. For recipe used in this study please refer Appendix Table A2.
- After sputtering for the designed time period, system is shut off and allowed to cool down. Both the motors are switched off and vacuum is vented to bring chamber to atmospheric pressure.

- As the chamber reach atmospheric pressure wafer is taken out and its thickness is authenticated using Alpha step profilometer.

3.2.3 Alpha-Step Profilometer

It is essential to check the thickness of the material coated on wafer to get desired functionality on to sensors fabricated. To authenticate the thickness of the material coated alpha-step profilometer is used. It is a stylus-based surface profiler to measure step heights of surfaces. Appendix B shows alpha-step profilometer used for this work.

Procedure for measuring thickness is:

- Place the wafer on the stage and gently push it.
- Bring the wafer in contact with stylus by raising stage.
- Once stylus touches the wafer press start. Here stylus gently dragged along the surface of the substrate. The vertical deflection measures the change in step height. Also drag length can be adjusted as required to know the uniformity.
- Change in the step height will be shown on the screen by plotting the lowest and highest point thickness of the material is read.

3.2.4 Spin Coating

Spin coating has been used for several decades for the application of thin films [47]. Spin coating is a process by which different film material of desired thickness can be deposited by spinning then on a wafer. A typical process for spin casting process is shown in Figure 17. Desired quantity of liquid is injected or poured onto the surface of a

wafer, which is attached to the wafer holder using vacuum. The wafer holder is attached to motor, which spins at required speed. Centripetal force causes liquid or resin to spread out and eventually form a uniform film onto wafer. Final film thickness and other properties will depend on the nature of the resin and the parameters chosen for the spin process. Factors such as final rotational speed, acceleration, and fume exhaust contribute to how the properties of coated films are defined [48]. The thickness of the film deposited depends on viscosity of material, time of spin and spin speed [18].

$$x \propto \frac{\eta f}{\sqrt{\omega}} \quad (5)$$

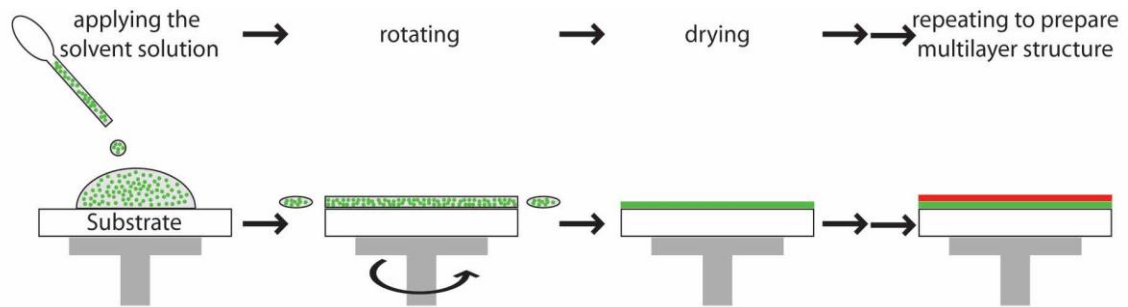


Figure 17 Spin coat process [49]

For current work Laurel resist spinner is used. Appendix B shows Laurel resist spinner used for this research. Procedure used for spin coating:

- Substrate after metallization is cleaned by rinsing in acetone followed by methanol rinse and deionized water, finally dried using compressed nitrogen.
- Substrate then is placed on the wafer holder (before this spinner has been cleaned to get rid of dust and other vapors) make sure wafer is approximately at the center to prevent uneven coating.

- Then Hexamethyldisilazane (HMDS) is spun on to wafer at known parameters. HMDS improves sticking of resist to ST-quartz.
- Allow HMDS to dry for few minutes this would avoid reverse reaction during developing.
- Finally resist selected (S1813 by microchem or SU-8 2035 by microchem) is spun at pre-determined parameters. If the resist is spun on to wafer as a waveguide then bonding pads are covered by kapton tape. This is done because if bonding pads are coated with resist then sensor would behave as capacitor and wouldn't respond to surface interactions.
- Wafer is removed from the spinner and soft baked for few minutes at temperatures in the range of $90^{\circ} - 120^{\circ}\text{C}$ depending on type of resist. Soft bake is done before exposure and developing just to strengthen resist adhesion to wafer, also it smoothens sharp bumps at the edge of wafer [41].
- Wafer is then allowed to cool slowly by keeping it on a metal plate. Recipe used for spin coating S1813 is shown in Table A3.
- After wafer is cooled to room temperature thickness of resist coating is checked using alpha step profilometer.

3.2.5 Photo Lithography

Lithography is the process of transferring mask pattern onto a thin layer of material called resist, which is a radiation-sensitive material. Exposure to UV radiation changes the solubility of resist in developer [50].

The pattern transfer is accomplished by using an instrument called mask aligner that emits UV radiation at desired power [51, 52]. The performance of the tool is determined by three properties: resolution, registration, and throughput. Resolution is defined as the smallest possible size in mask pattern that can be imprinted onto a resist film. Registration gives the accuracy of successive masks alignment with respect to the previously defined patterns on a wafer. Throughput gives rate of wafer exposure, which is the number of wafers that can be exposed per hour for a given mask. Depending on the resolution, several types of radiation (e.g. ultraviolet (UV) and X-rays) may be employed in lithography [18, 41, 53].

In optical lithography three different methods can be used for transferring the desired pattern on the photoresist. These three methods are shadow printing, proximity printing and projection printing [52].

In shadow printing mask is in direct contact with the wafer as shown in Figure 18 (a). This gives very high resolution. But often shadow or contact printing results in mask damage with time due to particles on wafer surface [52].

Proximity printing minimizes the mask damage. In proximity printing, patterns from mask are projected onto a resist-coated wafer. Here mask is placed few centimeters

away from the wafer as can be seen in Figure 18 (b). To increase resolution in proximity printing, only a small portion of the mask is exposed at a time [40, 52].

In projection printing mask and wafer are several inches away. To improve resolution an imaging optics is used between mask and wafer, this collects images from mask pattern and projects it on the wafer this can be seen in Figure 18 (c). Resolution can be varied by varying the distance of imaging optics [54].

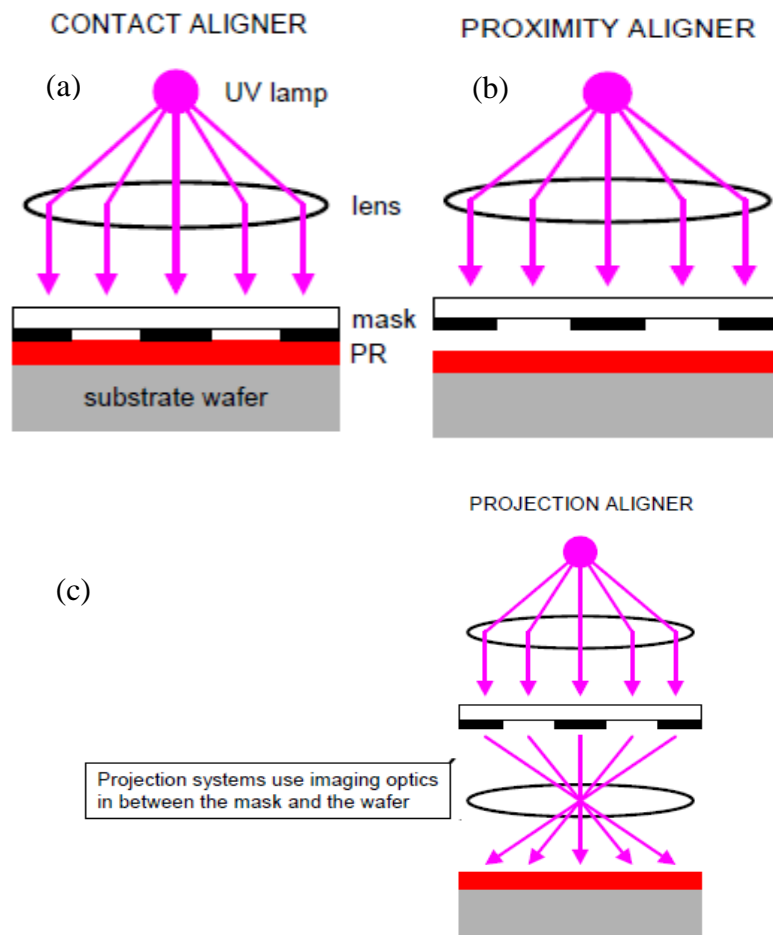


Figure 18 (a) Contact printing, (b) Proximity printing and (c) Projection printing [54]

For exposure in this work Karl Suss mask aligner is used and it is shown in Appendix B. Procedure adapted for current work is listed below:

- Soft baked wafer is cooled to room temperature and placed on the stage.
- Nitrogen to UV source is turned on this protects UV bulb from burning. Then motor for vacuuming the system chamber is switched on and finally mask aligner is turned on. Mask aligner is always used in constant power mode.
- Mask holder and chuck is replaced to match 3 inch wafer.
- Mask is cleaned with acetone, methanol, deionized water and nitrogen gas to remove dust and other particles and avoid mask from damaging.
- Mask is then clamped onto mask holder and aligned to match the wafer.
- Desired program is selected and UV lamp intensity is adjusted by varying the power. UV lamp is set to desired intensity using photo intensity indicator.
- Then based on the thickness and type of resist, suitable exposure time and type of resist (positive or negative) is selected for exposure.
- Contact printing is then selected for high resolution image.
- Followed by transferring mask on to chuck, is then clamped to the system and pressed start exposed. Recipe of photolithography used for this study can be found in Table A3.
- After the exposure step, wafer is carefully unloaded and another wafer is loaded for exposure.
- Exposed wafer later will be developed using an appropriate developer.

3.2.6 Developing

A resist is a radiation-sensitive material, which can be classified as positive or negative depending on its response to radiation exposure. The positive resist shows more solubility in a developer after it is exposed to radiation [52]. Therefore positive resist can be easily removed while developing. The patterns formed by the positive resist are the same as those on the mask. A negative resist shows less solubility in a developer after exposure to radiation. The pattern formed by a negative resist is the opposite of those on the mask patterns [41, 18]. Figure 24 shows difference between positive and negative resist.

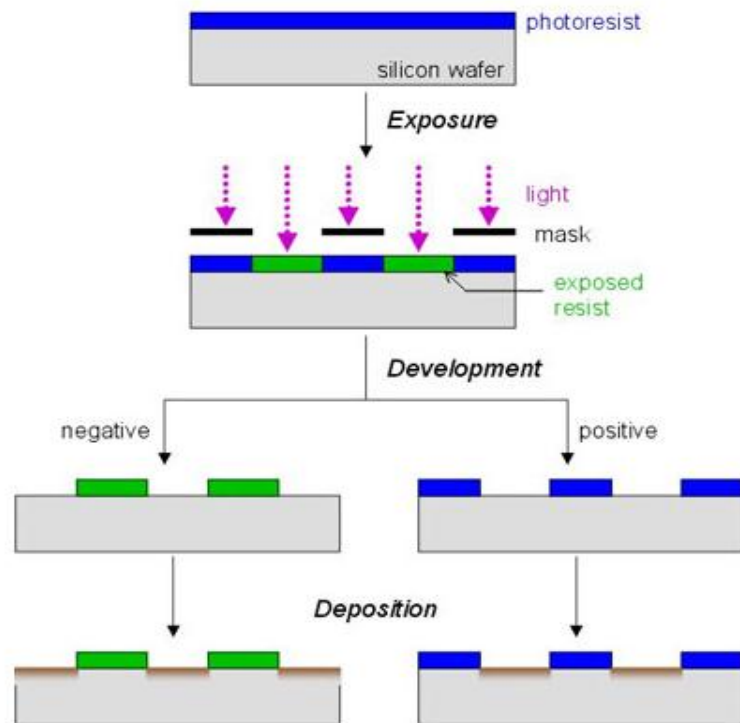


Figure 19 Difference between positive and negative resist [55]

Developing photo resist is very much similar to developing photos from negatives. Procedure followed for developing is listed below:

- First depending on the solubility type of resist, developer is selected (AZ726 or SU8 developer)
- Before exposure it is important to know the developing time. Again based on thickness, exposure intensity, type of resist and resist solubility developing time is selected. Typically it ranges from 1min to 10min at room temperature.
- Safety is especially important while using TMAH based developers, as its vapors are hazardous to eyes and skin. For TMAH based developers it is always suggested to wear nitrile glove, body cover and face shield.
- After all the safety measures, developer is carefully poured into specifically dedicated beakers for developers, since mixing of developer might lead to some caustic reactions.
- Wafer with exposed side facing upward is immersed in the developer and timer is started simultaneously. While immersed, by orienting the sample properly under the chemical desk light user can see how interference patterns fluctuate on the resist, first revealing the patterns and then making them disappear, and showing up again when the development progresses. After a while the fluctuation ceases when the resist thickness becomes less than needed for interference in range of visible light. The first estimate for optimal development time is often taken by adding 15 seconds to the time needed to

make the fluctuation to disappear [53]. Refer to Table A3 for recipe used in this work.

- Once developed ST-quartz is taken out, rinsed with deionized water and dried using compressed nitrogen, to remove photoresist and developer floating on the wafer surface.
- Later developed ST-quartz is examined under compound microscope to check the resolution and uniformity in developing.
- Once wafer is fully developed, it is hard baked between the temperature range of 100°C to 160°C for 15 to 30 minutes in a convection oven, depending on type of resist. Baking significantly improves chemical resistance and adhesion properties of the resist to the wafer [55].

3.2.7 Wet Etching

Wet etching is a material removal process by chemical reaction between etchant and material being etched. It uses liquid chemicals as etchants to remove materials from a wafer. The desired patterns are protected by the photoresist on the wafer, while unprotected areas on the wafer are etched away [56, 18].

A wet etching process involves multiple chemical reactions. The wet etch process can be described by three basic steps [57].

- Diffusion of the etchant onto the material that is to be removed.
- The chemical reaction between the material etched and the liquid etchant.

Typically it's a reduction-oxidation (redox) reaction.

- Diffusion of the chemical reaction product from the reacted surface [57].

Procedure used to etch chrome in this work is as follows:

- Always use plastic or fiber wafer holder, while metal etching.
- Pay special attention to safety, since chrome etchant is corrosive it's highly advisable to wear all the safety gears available.
- Before etching, always make sure to conduct glove test checking for potential holes in gloves. Discard those gloves if holes are observed.
- After wearing all the safety gears take out the chrome etchant from box and pour it to the glass bowl carefully.
- Immerse quartz wafer completely in chrome etchant with etch rate 500^oA/ min and continue etching until no traces of chrome on the wafer except on the protected pattern is observed.
- After etching process is completed, rinse the wafer thoroughly with deionized water leaving no trace of chrome etchant on the wafer.
- Finally strip the photoresist from the wafer using photoresist stripper and rinsing with acetone, methanol, deionized water and drying with compressed nitrogen gas to remove possible contaminant from the surface.

3.2.8 Waveguide Deposition

Love wave sensors employ waveguides that have shear velocity less than that of wafer on the surface, to confine acoustic wave to surface of wafer. Described here are processes used for depositing guiding layers SU8-2035 and SiO₂ on quartz substrate.

3.2.8.1 Spin Coating (SU8-2035)

Same procedure as discussed above is followed to spin coat SU8-2035 onto etched quartz. Before spin coating bonding pads are protected using kapton tape, since property of sensor change with SU8 on bonding pads. SU8- 2035 is spun on to the wafer using spinner. Recipe for SU8-2035 spin coating is given in Table A3. Once resist is spun on quartz wafer. Wafer is then soft baked at 90°C to 100°C for around 2 to 5minutes. Soft baked wafer is then exposed at desired UV lamp intensity using Karl-Suss mask aligner. Before exposure the mask is aligned to the wafer and system is set to expose negative resist. After exposure, SU8 is developed using SU8 developer for around 4-10min at room temperature. Developed SU8 is later hard baked for 15 to 30 minutes at 140 to 150°C in convection oven to get glossy SU8 waveguide on quartz.

3.2.8.2 Plasma Enhanced Chemical Vapor Deposition (PECVD)

Plasma Enhanced Chemical Vapor Deposition (PECVD) is an alternative method for depositing thin films at lower temperature without compromising quality of film deposited [58].

Basic principle of PECVD process is glow discharge generated using electrical energy is transferred to the gas mixture in the chamber. This gas mixture has all the elements needed for deposition. Using the energy transmitted gas mixture transform into reactive radicals and ions. These fragments interact with substrate and form deposition. Since reaction occurs at gas phase, substrate can be maintained at lower temperate when

compared to other chemical vapor deposition process [59, 60, 61]. Figure 20 shows basic working of PECVD process.

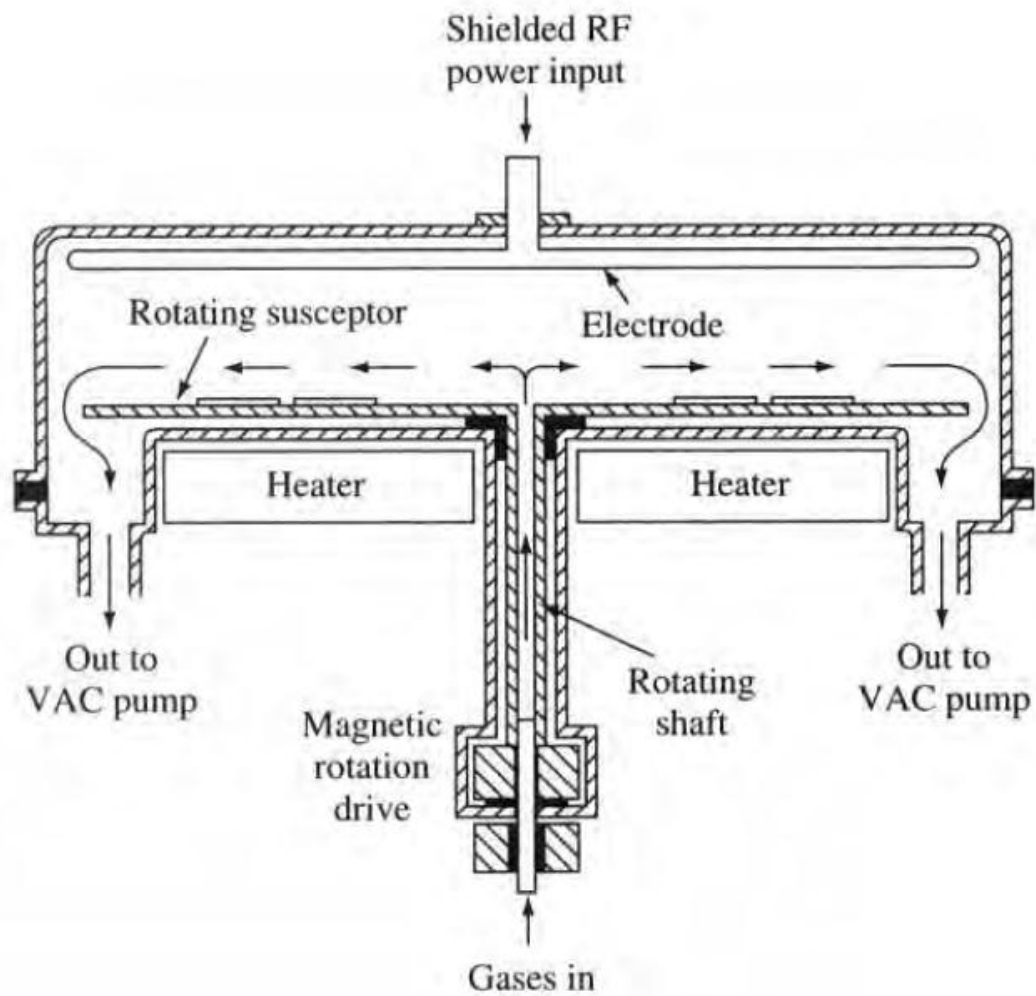


Figure 20 Typical PECVD process [18]

Here is the procedure followed for depositing silicon dioxide SiO_2 on ST-quartz:

- Etched and cleaned wafer is placed inside PECVD reactor.
- Chamber should be well cleaned before installing wafer to the PECVD.
- Power to the reactor is turned on.

- This switches on motor, heater and power source to the system.
- Turn on the N₂O gas supply (99.99% pure) to the chamber.
- Before the actual deposition surface pre deep cleaning is done for few minutes. This will coat thin film on the inside surface of the reactor, this would avoid contamination of chamber in the later stage. Recipe used for pre cleaning is given in Table A4.
- Then in deposition stage Silane (SiH₄) and N₂O flow is turned on, this gas mixture undergo reaction when glow discharge is transmitted. Reactant produced (SiO₂) gets deposited on quartz. Recipe used for deposition is given in Table A4.
- Power to the system is turned off and system is allowed to cool down for few minutes.
- Wafer is taken out and cleaned by rinsing with acetone, methanol and deionized water and compressed nitrogen to dry wafer.

3.2.9 Dicing Saw

Dicing saw is the instrument which cuts wafer into desired individual chip. This is done using a thin blade, which is exclusive for type of wafer selected. Using dicing saw any size wafers can be cut. Dicing parameters are selected based on the geometry and thickness wafer. Wafer parameters are programmed in to dicing saw to cut the wafer into required shape and size [18, 41].

Procedure for dicing quartz substrate is explained below and dicing saw used for this work shown in Appendix B.

- Mount wafer on hot plate of wafer tape applicator with pattern facing downward. Apply tape on backside of wafer and cut tape to desired size using knife on tape applicator. This process prepares wafer for dicing saw.
- Mount diamond tip hub less blade onto the dicing saw machine
- Turn on air and water flow, followed by micro-automation dicing saw machine.
- Once spindle start rotating at full speed, place wafer on the stage and turn on the vacuum. This holds wafer firmly on the stage.
- Press program button on the panel to enter wafer parameters to the system, this determines the speed of cut, height of cut, length of cut and movement of blade after each cut. Recipe for dicing saw is given in Table A5.
- Set spindle to prescribed speed, otherwise blade will break.
- Use camera to align dicing line to blade and press single cut to start dicing.
- Use up and down arrows in align mode to move blade to next position.
- To dice at the desired angle press counter clockwise button in align mode to rotate wafer and then single cut to start dicing.
- After dicing, take out wafer carefully and discard all the remains of wafer.
- Finally clean wafer by rinsing in acetone, methanol and deionized water and dry with nitrogen gas to remove all dust and other particles from diced wafer surface.

3.3 Sensor Preparation

Sensor preparation is a very important procedure. Here it is where diced wafer becomes complete sensor by making electrical connections.

Procedure followed for sensor preparation is given below:

- Diced wafers are separated and mounted on circuit board using double sided sticker.
- Wire is cut into desired length, bent and soldered onto sensor.
- Silver epoxy is mixed with resin in 100:3.4 ratio and used on bonding pad to make electrical connection. This is allowed to solidify for 24 hours.
- After solidification sensor is connected for signal generation and detection. This is plugged into network analyzer and tested at variable temperature.

Figure 21 shows complete sensor with all electrical connection.

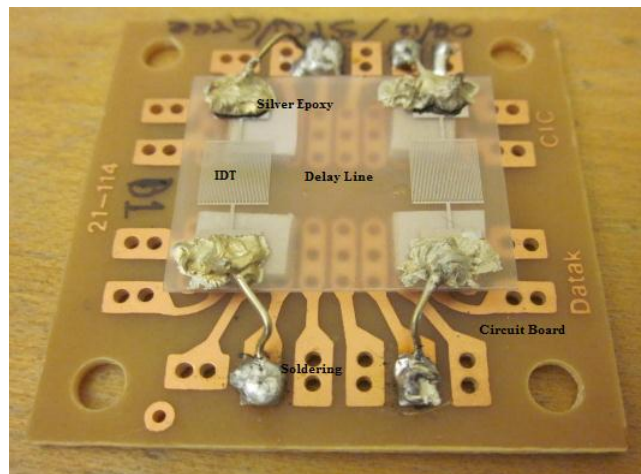


Figure 21 Sensor connection

3.4 Testing Instruments

Designed and fabricated sensors need to be tested for their ability to perform as designed. This evaluation is conducted with variety of electronic instruments which aids in generating and detecting signal from the sensor. Data acquired is analyzed for quantifying sensor performance.

3.4.1 Network Analyzer

Network analyzer is an instrument used to analyze electrical performance of the components and circuits used in complex system. Network analyzer is capable of measurement at wide range of frequencies [62]. Typically network analyzer is used to measure scattering parameters (S-parameter), by measuring the input and output signal distortion effect on amplitude and phase of frequency [63].

Basic fundamental principle of network analyzer is the measurement of reflected, incident and transmitted energy from the device being test. When a wave travels through a network, its logarithmic magnitude (logmag) and phase change due to scattering thus giving the resulting output wave. S-parameter can be considered as gain of the network and subscripts denote the port number [64]. Figure 22 illustrate the basic working principle of network analyzer and importance of each signal.

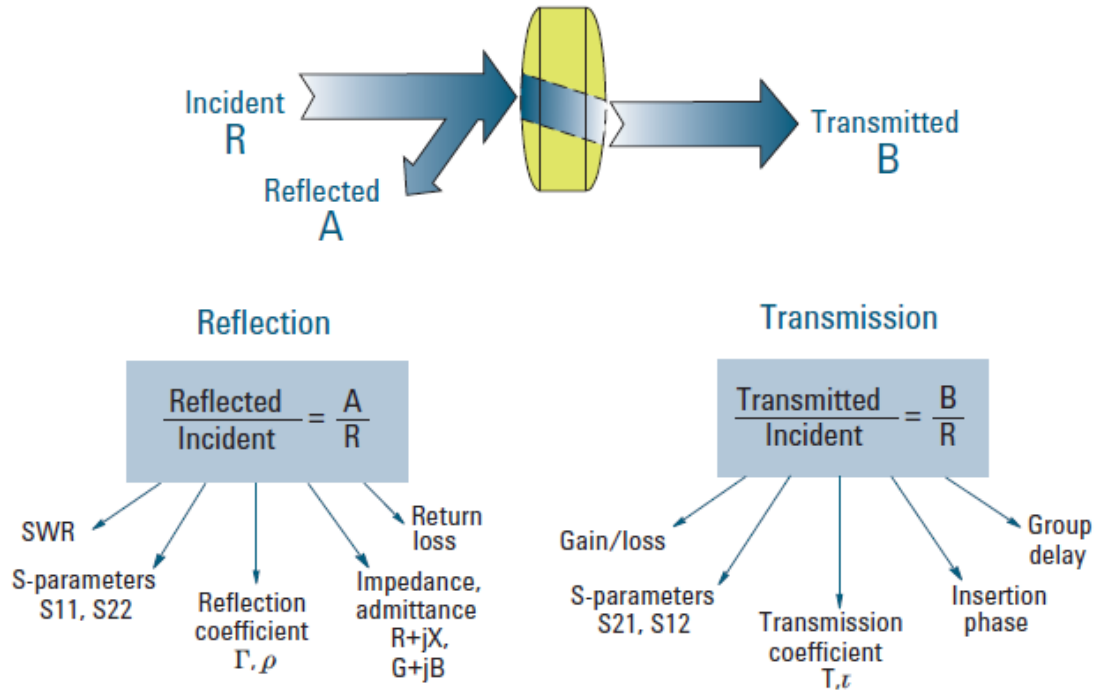


Figure 22 Basic working principle of network analyzer [64]

3.4.2 Multi-meter

Multi-meter is a device that combines the functionality of many instruments into one compact unit. A typical multi-meter measures voltage, current, temperature, capacitance and resistance. Multi-meter costs from less than \$10 to more than \$5000. Also multi-meter is available in analog and digital form [65]. The specific multi-meter employed in this study is illustrated in Appendix B.

3.4.3 Convection Oven

Convection oven is an oven that imparts heat assisted by force of air. This movement of air helps to reach higher temperature quickly and keeps the temperature stable at desired point. The air circulation or convection tends to eliminate hot spots

creating uniform temperature throughout the chamber [66]. Figure 23 shows basic working principle of convection oven used for this work.

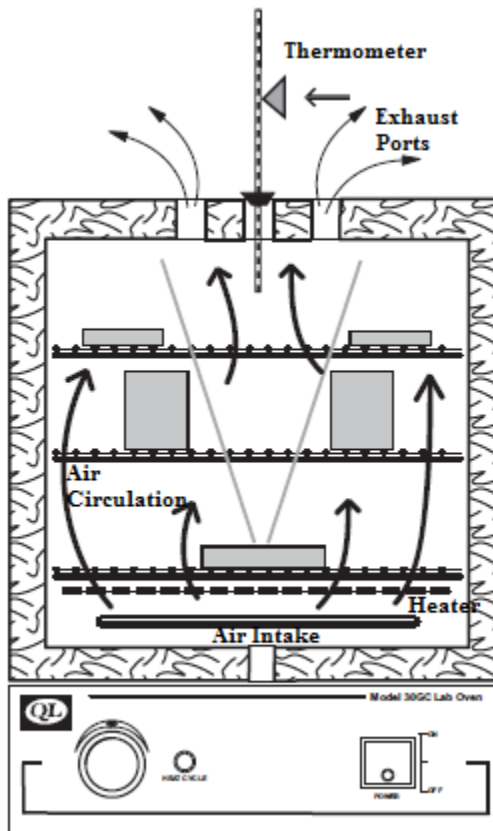


Figure 23 Convection oven principle [67]

3.5 Experimental Setup

Objective of this research is measuring temperature variation using different SAW device designed and setup used for measuring is shown in Figure 24.

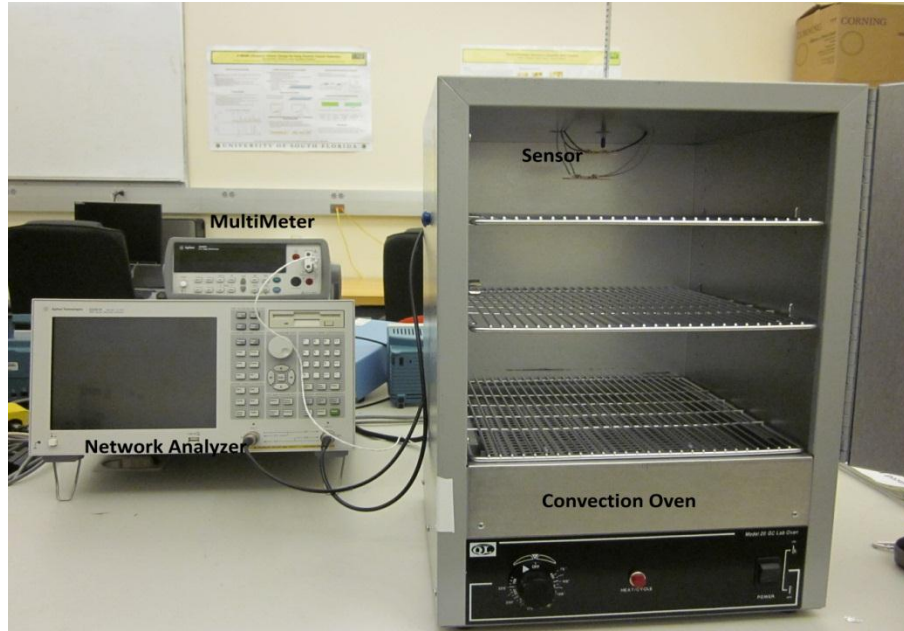


Figure 24 Experimental setup

Whole process of generation and detection of sensor signal is conducted in the setup illustrated in Figure 24. Process details are explained below:

- Place the sensor in the convection oven made by Quincy lab Inc. model 20 GC which can operate at a temperature range $30^{\circ}\text{C} - 450^{\circ}\text{C}$ with an accuracy of $\pm 6^{\circ}\text{C}$.
- Temperature inside oven is measured using thermometer and digital multi-meter by Agilent technologies E5061A with an accuracy of $\pm 0.01^{\circ}\text{C}$. Temperature probe from multi-meter goes through oven which gives real time temperature for testing sensor.
- Connect sensor to 2 port network analyzer Agilent technologies E5061A with an operating frequency range of $300\text{ kHz} - 1\text{ GHz}$ and turn on oven, multi-meter and network analyzer.

- Before taking measurement, network analyzer has to be set to desired condition to excite surface wave.
- Network analyzer frequency should match frequency of the sensors designed to excite acoustic wave. In this work sensors are designed to work at 17 MHz and network analyzer is set at a range of 16 MHz – 18 MHz using start and stop option on the network analyzer.
- Under stimulus in network analyzer, sweep setup is used to set number of point in plot. Higher the number of points, higher the resolution. Maximum points that can be set in this network analyzer and also used for this study are 1600.
- To set input and output for sensor, go to measure under response menu in network analyzer. There are 4 options available S11, S12, S22 and S21. This allows user to measure ratio of different combination of incident, reflected and transmitted wave called S-parameter. For this study S12 is measured, which is the ratio of output of port 1 to the incident wave on port 2.
- In the same menu under response – format is used to select the type of sensor response to be measured. For this study logarithmic magnitude and phase of the attenuated signal is measured while changing the temperature.
- To set the sensor response centered on the screen auto scale option under response – scale is selected.
- Sensor response showed more noise in signal, this is minimized by selecting option under response – average. This reduces noise by averaging the response.

- Finally after averaging, sensor response as logarithmic magnitude and phase is recorded using saves and recall under instrument state menu. Data is recorded for every 5°C increment from 30°C±0.5 to 80°C±0.5.
- Data recorded will be in Microsoft excel format which is later used for analysis.

3.6 Data Analysis

Data analysis is an important part of any research. Here raw data is converted to useful information. This is done using Matlab or Microsoft Excel along with some set of formulas.

Data acquired from network analyzer is in Microsoft Excel format. This raw data is used to plot sensor response as logarithmic magnitude and phase on y-axis and variable temperature on x-axis. This allowed identification of the peak sensitivity for a sensor. Later this peak is studied for surface perturbation caused by change in temperature and plot combining sensor response for every temperature interval is recorded.

Due to surface perturbation, velocity and amplitude of the wave change results in a frequency shift of the peak. This frequency shift is calculated at every interval of temperature using the formula:

$$\Delta f = f_1 - f_n \quad (6)$$

where Δf stands for frequency shift at given temperature, f_1 for frequency response at lowest measured temperature and f_n is frequency response at every temperature interval.

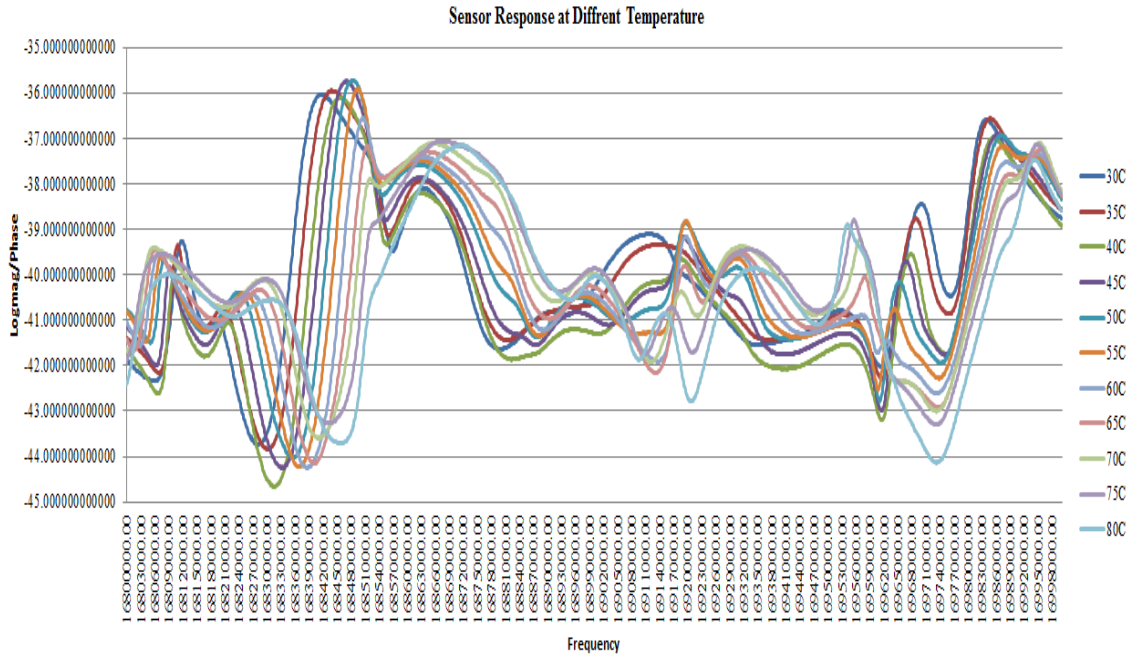


Figure 25 Sensor response at different temperature

Figure 25 shows a typical sensor response recorded using network analyzer at different temperature conditions. Every peak in the response is studied and one with better frequency shift for temperature change is used for analyzing sensor performance.

Frequency shift calculated for logarithmic magnitude and phase is plotted against temperature to analyze performance of designed sensors, which is discussed in next chapter.

4. Results and Discussion

This section discusses experimental results obtained with different sensor configurations investigated and performance comparison between sensor types.

Comparison is drawn between sensors by plotting frequency shift of logarithmic magnitude and phase as y co-ordinate and temperature as abscissa. Using linear trendline for the data plot as a reference, sensors are analyzed and compared.

4.1 Comparison of In-house Sputtered and Outside Sputtered Sensors

In this section in-house sputtered, that is quartz wafer sputtered in Nanotechnology Research and Education Center (NREC) using CRC sputtering machine and outside sputtered that is quartz wafer sputtered from a commercial vendor (University Wafer, South Boston, MA) are compared.

4.1.1 Comparison of Bi-directional Electrode Sensors

Figure 26 illustrates frequency shift of logarithmic magnitude and phase for temperature ranging from 30°C to 80°C for in-house bi-directional IDT configuration. It can be inferred from Figure 30 that for every 5°C increment in temperature there is a response change observed from the sensor. This indicates that the designed and

fabricated sensor is successfully responding to the surface perturbation. One can observe from this figure that logarithmic magnitude shift indicates higher sensitivity to change in temperature than phase shift. This result is drawn by observing slope for linear trendline. However by observing linear regression (R^2) value which ranges from 0 to 1 it can be inferred that phase shift has more linearity regression compared logarithmic magnitude shift.

Figure 27 shows frequency shift of logarithmic magnitude and phase for outside sputtered bi-directional IDT configuration. This sensor is tested under same condition used for in-house sputtered sensor.

From this figure it can be clearly inferred that phase response is more sensitive to change in temperature compared to logarithmic magnitude and linearity remains to be approximately same for both logarithmic magnitude and phase shift.

When outside sputtered bi-directional sensor is compared with in-house sputtered bi-directional sensor configuration, it can be observed that outside sputtered sensor show higher sensitivity for both logarithmic magnitude shift and phase shift than in-house sputtered. Also it can be clearly observed that linearity is near one for outside sputtered sensor, meaning sensor response follows linear uniform shift for every temperature measurement.

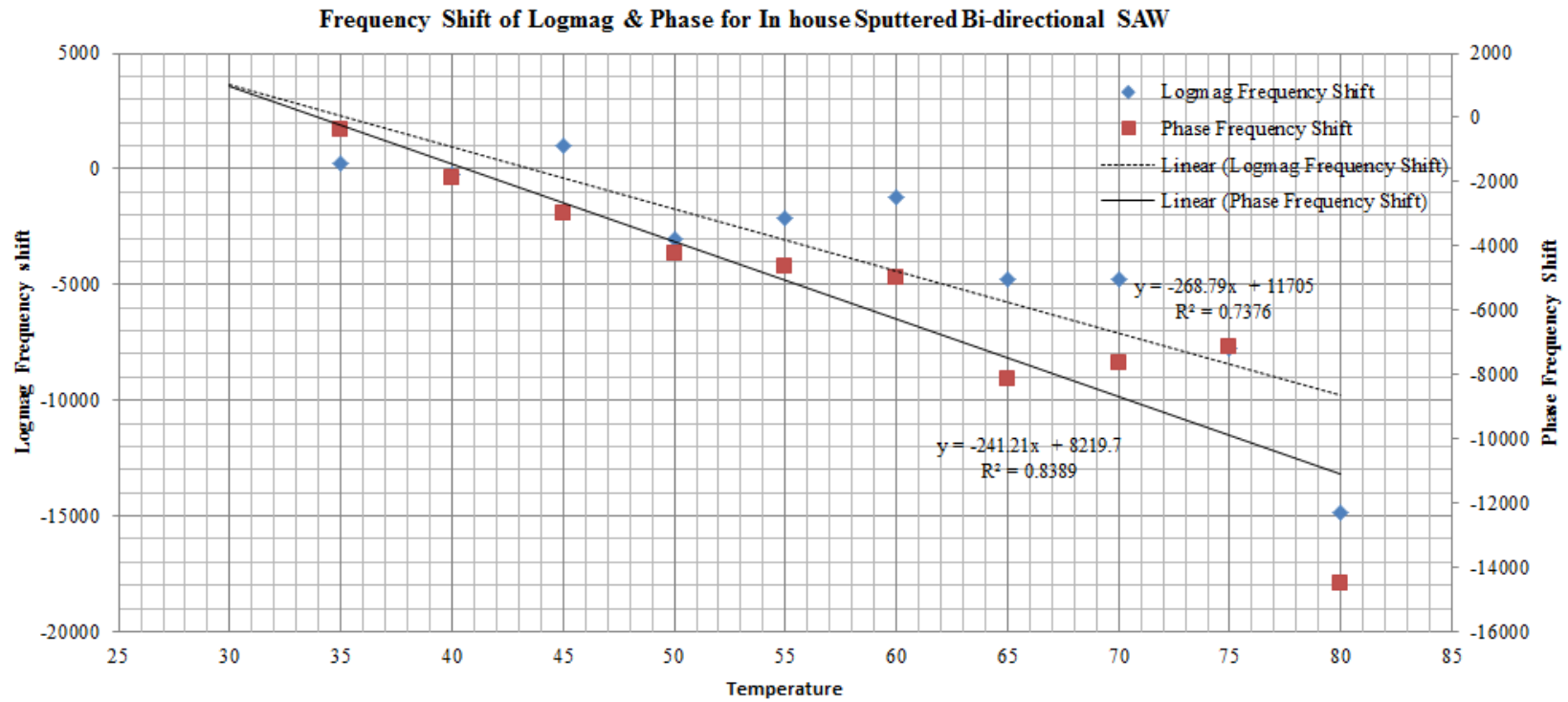


Figure 26 Frequency shift for in-house sputtered bi-directional IDT sensor

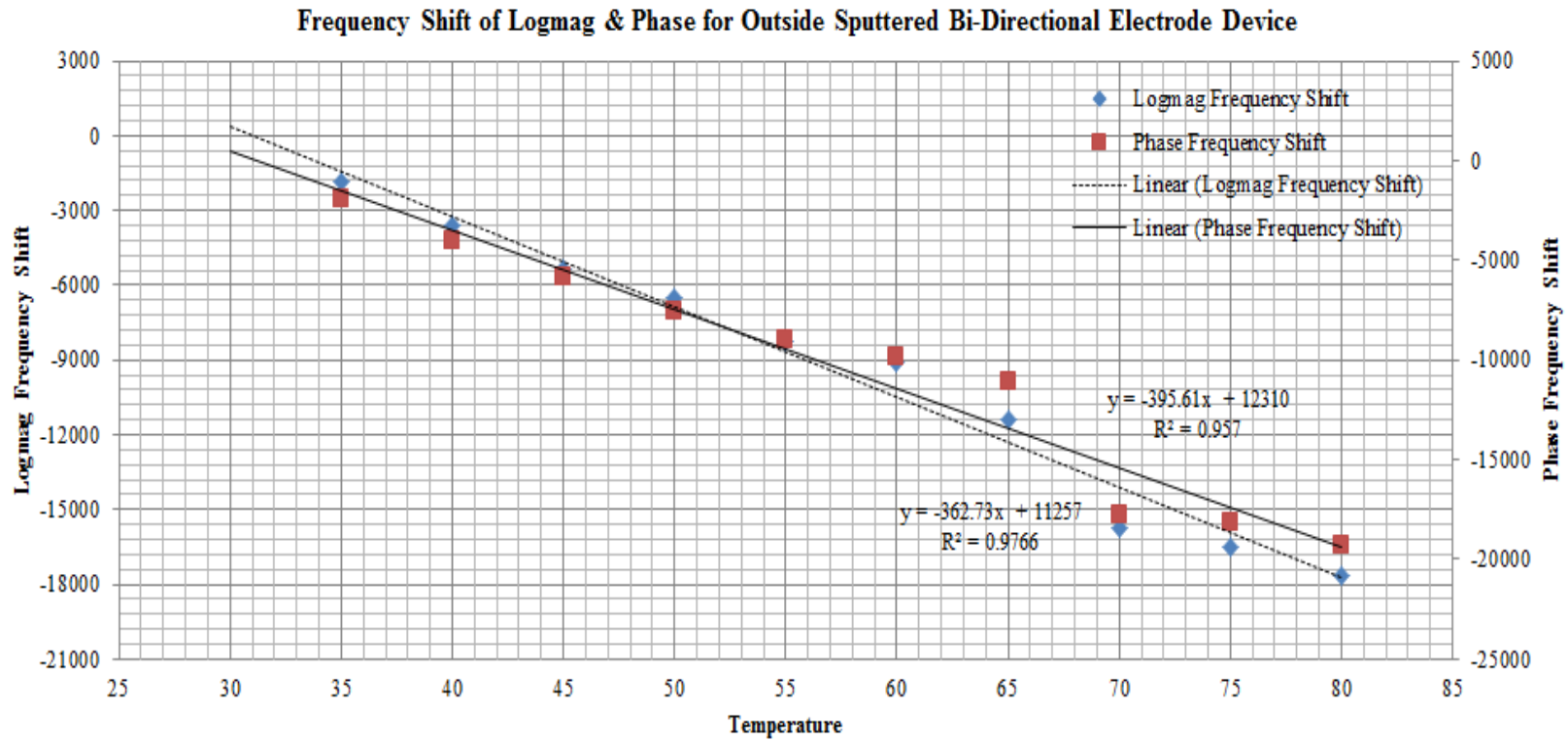


Figure 27 Frequency shift for outside sputtered bi-directional IDT sensor

4.1.2 Comparison of Split Electrode Sensors

It has been reported that split electrode configuration reduces loss, signal reflection and noise, leading to increased sensitivity [37]. However it should be noted that sensitivity is also a function of electrode type, number of fingers, width and pitch of finger, delay path length and substrate selection.

Figure 28 illustrates logarithmic magnitude and phase shift of in-house sputtered split electrode sensors. It can clearly be observed from this plot that phase is more sensitive to change in temperature as compared to logarithmic magnitude. Also linear regression is almost 1 for phase shift.

Figure 29 illustrates logarithmic magnitude and phase shift for outside sputtered split electrode sensor. It can be seen that similar trend is followed as in Figure 32. Phase is more sensitive to perturbation and also phase shift is more linear than logarithmic magnitude shift.

When outside and in-house split electrode sensors are compared, outside sputtered sensor demonstrate twice the sensitivity when compared to in-house sputtered split electrode sensor. Linearity in frequency shift is approximately same for both sensors. But for both in-house and outside sputtered split electrode sensors logarithmic magnitude response showed poor linearity compared to phase response. Also it can be determined from graph that phase shift was more responsive to temperature for both in-house and outside sputtered split electrode sensors.

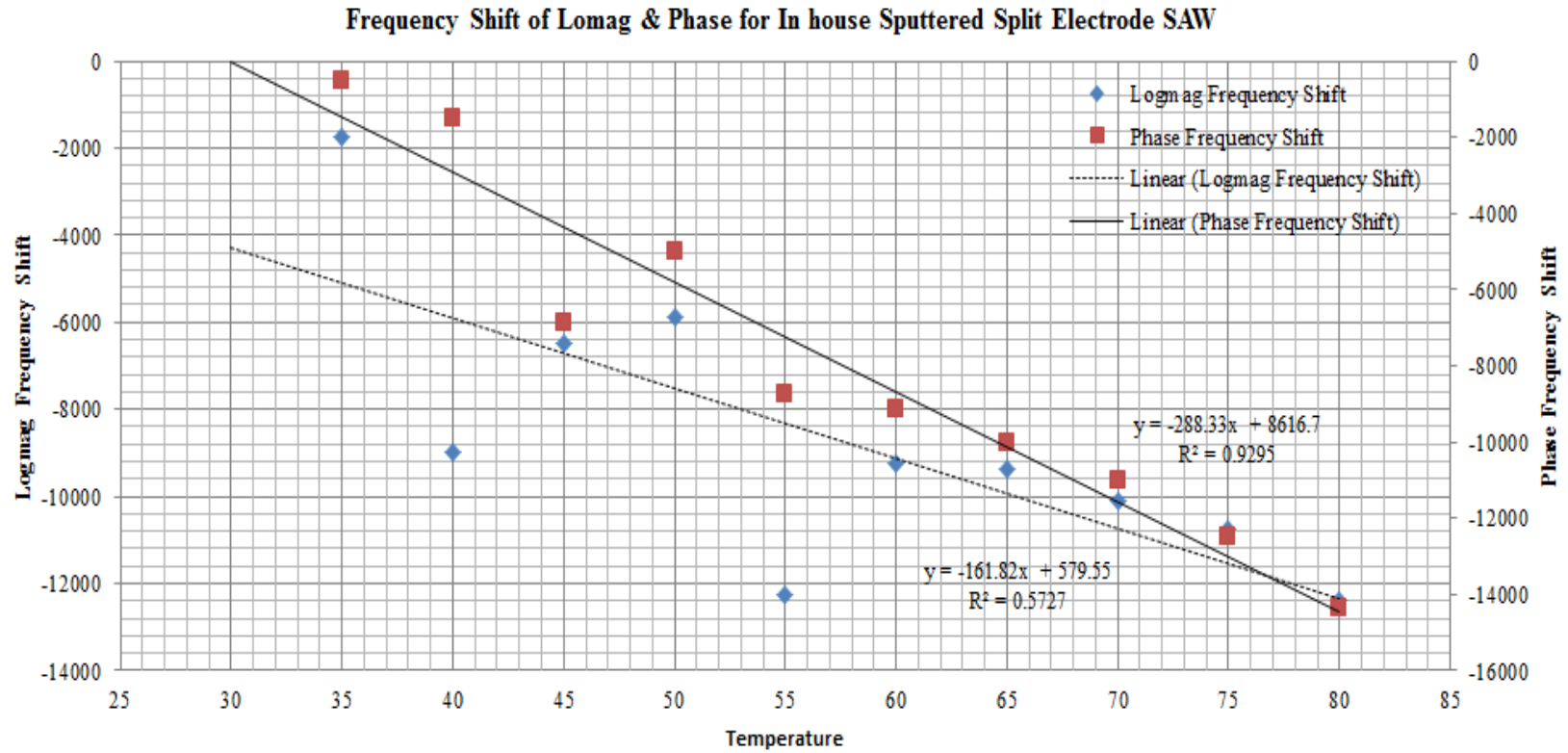


Figure 28 Frequency shift for in-house sputtered split electrode sensor

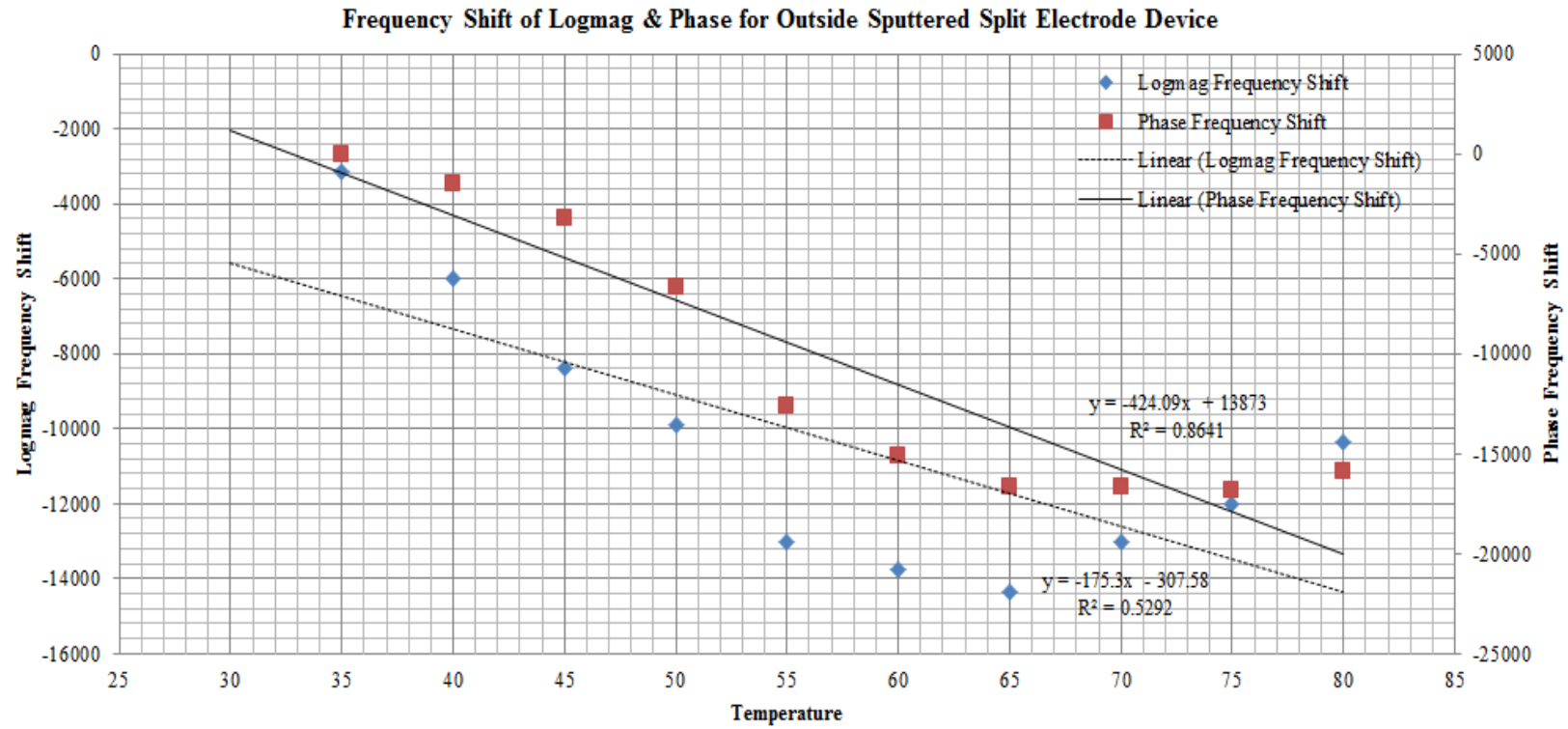


Figure 29 Frequency shift for outside sputtered split electrode sensor

4.1.3 Comparison of STW Sensors

Surface transverse wave sensors are sensors with metal grating on the delay line. This grating confine acoustic wave on the surface thus increasing sensitivity to surface perturbation.

Figure 30 illustrates the frequency shift for in-house sputtered STW sensor. Logarithmic magnitude here showed higher sensitivity to temperature as compared to phase. But both phase and logarithmic magnitude shift show relatively lower linearity with frequency shift varying all through the temperature change and this is due to reflection of signal in the grating.

Figure 31 illustrates frequency shift results for outside sputtered STW sensor. Again here logarithmic magnitude is more responsive to temperature change. Linearity in frequency change for both logarithmic magnitude and phase is comparatively good and approximately same.

When in-house STW sensor and outside STW sensor are compared, in house STW sensor showed higher logarithmic magnitude shift with sensitivity twice higher compared to outside sputtered STW sensor. But linearity in frequency shift is more uniform in outside sputtered STW sensor with linear regression almost equaling one. It can be also observed that in both the cases logarithmic magnitude shift was more responsive to temperature change.

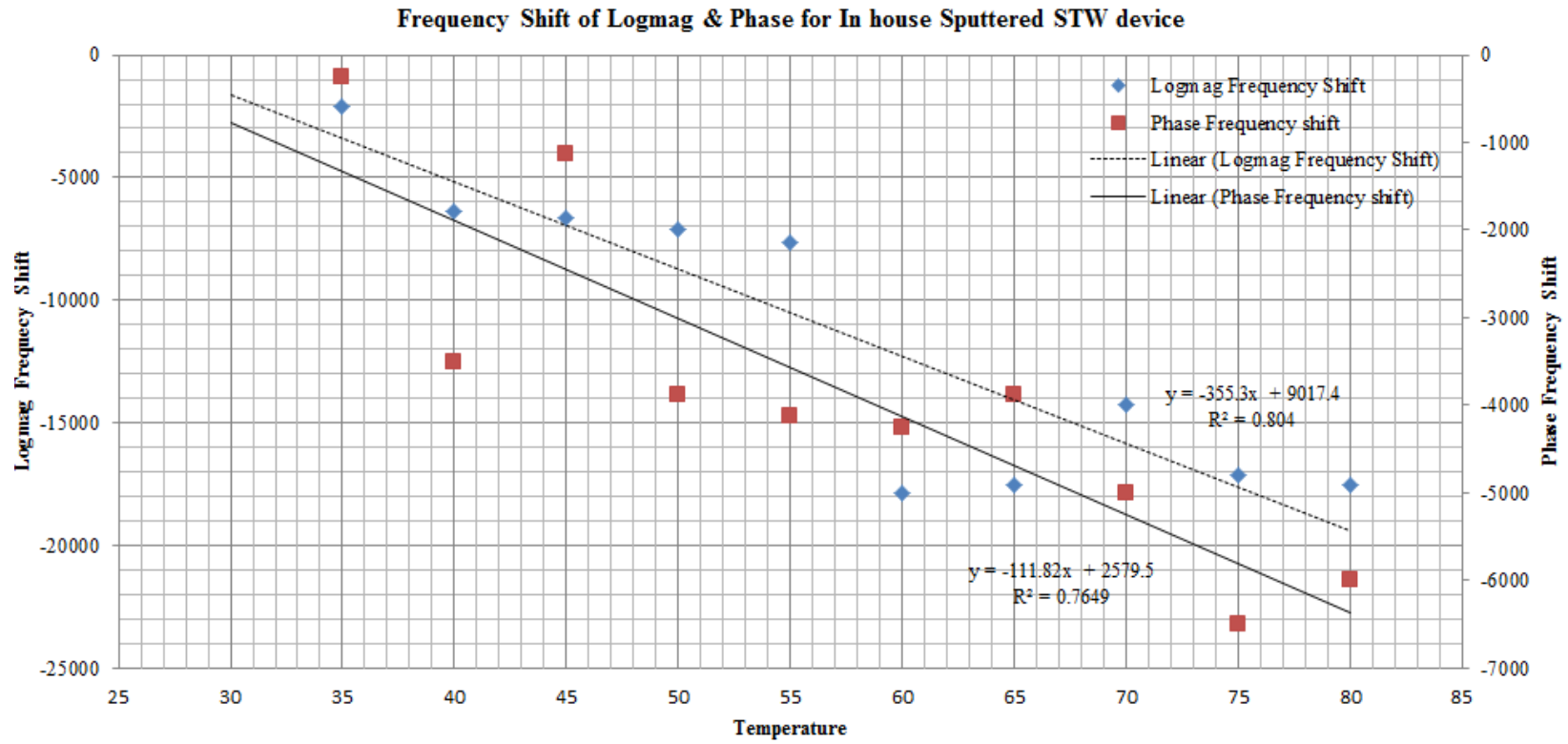


Figure 30 Frequency shift for in-house sputtered STW sensor

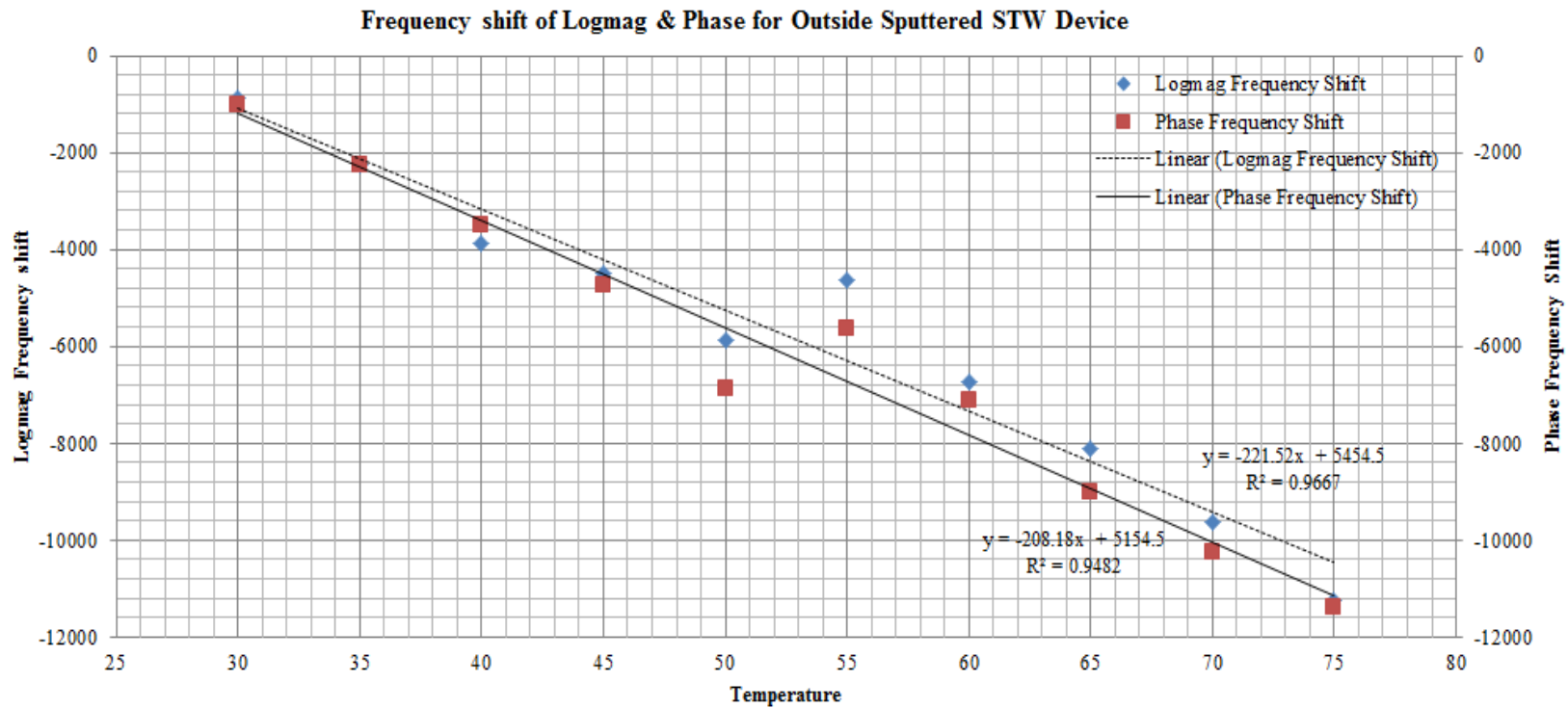


Figure 31 Frequency shift for outside sputtered STW sensor

4.1.4 Comparison of SPUDT Sensors

Sensor with single phase unidirectional transducer (SPUDT) is reported to have low reflection and low insertion loss leading to better sensitivity to surface perturbation [37].

Figure 32 is the plot showing frequency shift for in-house sputtered SPUDT sensor. Here phase has illustrated higher response to temperature change than logarithmic magnitude. It can be seen from plot that logarithmic magnitude relatively showed lower linearity. Frequency shift trend changed all through the span of temperature change.

Figure 33 showing frequency shift for outside sputtered SPUDT sensor. It can be clearly observed that SPUDT had shown very high sensitivity and uniform linearity for both phase and logarithmic magnitude all through the temperature range investigated.

When in-house sputtered SPUDT sensor and outside sputtered SPUDT sensor are compared, it can be clearly observed that outside sputtered SPUDT sensor show superior performance than in-house sputtered SPUDT sensor. Outside SPUDT sensor has shown twice the sensitivity when compared to in-house SPUDT sensor. Also when linearity of frequency shifts are compared outside sputtered SPUDT sensor showed almost perfect linearity with linear regression value approximately equaling one, which gives the measurement of uniformity in frequency shift for logarithmic magnitude and phase with temperature change.

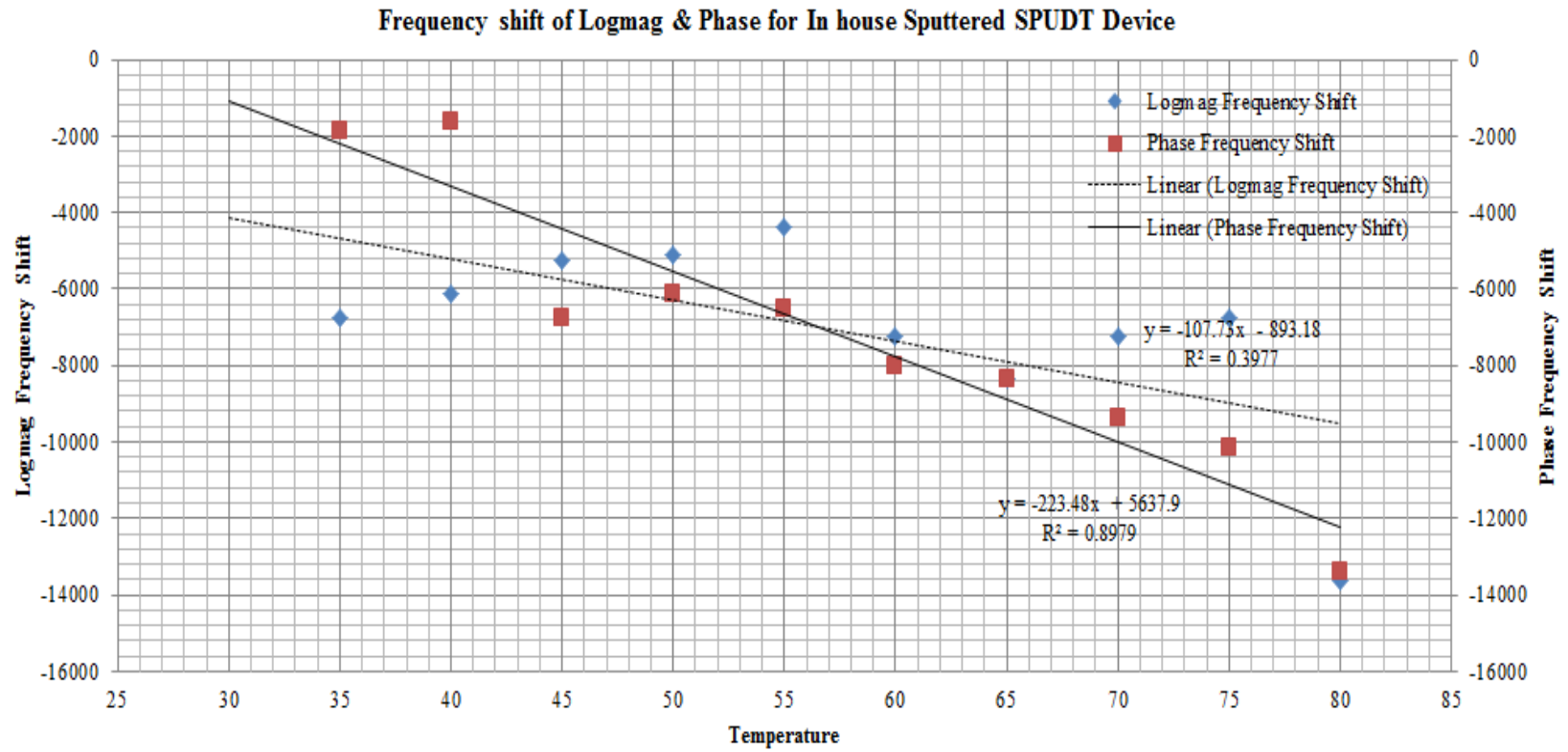


Figure 32 Frequency shift for in-house sputtered SPUDT sensor

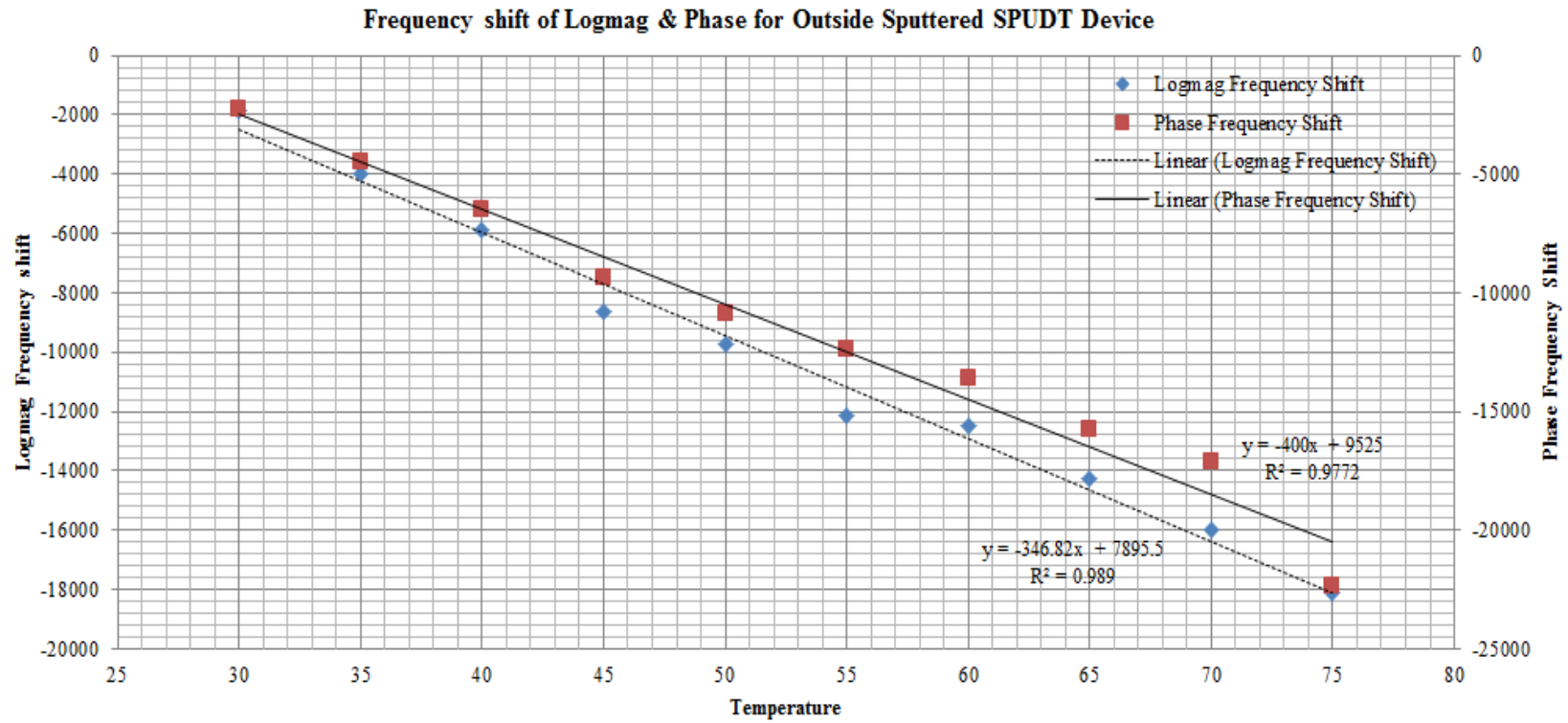


Figure 33 Frequency shift for outside sputtered SPUDT sensor

4.1.5 Summary

Table 2 Comparison of in-house and outside sputtered sensors

Sensor/Format		Logarithmic Magnitude		Phase	
		Equation	R ²	Equation	R ²
In House Sputtered	Bi-directional	Y= -268.7x+11705	0.7376	Y= -241x+8219.70	0.8389
	Split Electrode	Y= -161.8x+579.55	0.5727	Y= -288.3x+8616.7	0.9295
	STW	Y= -355.3x+9017.4	0.8040	Y= -111.8x+2579.5	0.7649
	SPUDT	Y= -107.7x+893.18	0.3977	Y= -223.5x+5637.9	0.8978
Outside Sputtered	Bi-directional	Y= -363.7x+11257	0.9766	Y= -395.6x+12310	0.9570
	Split Electrode	Y= -175.3x-307.58	0.5292	Y= -424.1x+13873	0.8641
	STW	Y= -221.5x+5454.5	0.9667	Y= -208.1x+5154.5	0.9482
	SPUDT	Y= -346.8x+7895.5	0.9890	Y= -400x+9525.00	0.9772

Table 2 gives summary for in-house and outside sputtered sensors. From the table it can be clearly observed that, of the entire in-house sputtered sensors bi-direction sensor configuration showed higher stability and linearity for both logarithmic magnitude and phase. When compared individually STW sensor configuration illustrated higher sensitivity and linearity to logarithmic magnitude with temperature change. When phase response is compared among in-house sensor configurations split electrode sensor configuration showed highest sensitivity as well as linearity with temperature change.

For outside sputtered sensors, bi-directional and SPUDT sensors showed very high response for both logarithmic magnitude and phase with change in temperature. Linearity for both the sensors showed to approximately one.

When in house and outside sputtered sensors are compared, it can be observed that outside sputtered sensors clearly are the foremost sensors of all except for STW sensors. Also outside sputtered sensors comparatively showed better linearity and stability for all sensors with change in temperature.

4.2 Comparison of Love Wave Sensors with SU8 and SiO₂ as Waveguide

Love wave sensors are surface acoustic wave sensors with a waveguide in their design. For Love wave sensors, waves are confined on the waveguide which improves its sensitivity to surface perturbation and protects IDT from being vulnerable to liquid sensing [68].

This section investigates about Love wave sensors with 2 different waveguides. Here outside sputtered wafers are used for fabricating love wave sensors as it comparatively showed better response to temperature. For this work SU8 and SiO₂ are used as wave guide. SU8 of thickness 40 μ m is spin coated on to the wafer and SiO₂ of 6 μ m is coated using plasma enhanced chemical vapor deposition. In this work 4 different sensors with 2 different waveguides are tested and compared.

Data obtained from network analyzer is plotted for logarithmic magnitude shift and phase shift on y-axis and temperature on x-axis. Frequency shift with respect to temperature is analyzed using these plots.

4.2.1 Comparison of Bi-directional Electrode Love Wave Sensors

Figure 34 shows frequency shift of logarithmic magnitude and phase for SU8 coated bi-directional electrode sensor. It can be inferred from the graph that phase shift is more prominent than logarithmic magnitude for temperature. Frequency shift for both logarithmic magnitude and phase show similar linearity. But it can be observed that frequency shift is positive for SU8 which is contradictory to frequency shift in other sensors tested. This is due to viscoelastic behavior of the polymer SU8 [69]. At lower temperature SU8 behaves as a rigid material displaying elastic behavior. As temperature increases deformation of SU8 occurs and material softens showing viscous behavior [70].

Figure 35 show frequency response of logarithmic magnitude and phase for SiO₂ coated bi-directional electrode sensor. It can be from this figure that phase is more responsive to change in temperature than logarithmic magnitude. With SiO₂ as waveguide, sensor showed good linearity for phase shift.

On comparing different waveguides for bi-directional sensor, it can be observed that SU8 love wave sensor showed much higher sensitivity than SiO₂ sensor but frequency shift for SU8 love wave sensor went in positive direction which is contradictory to frequency shift in SiO₂ love wave sensor. This is mainly due to viscoelastic effect in SU8 polymer. Also SU8 love wave bi-directional sensor showed slightly higher linearity when compared to SiO₂ love wave bi-directional sensor. It can be observed from the figure that phase shift is more responsive for both the waveguides.

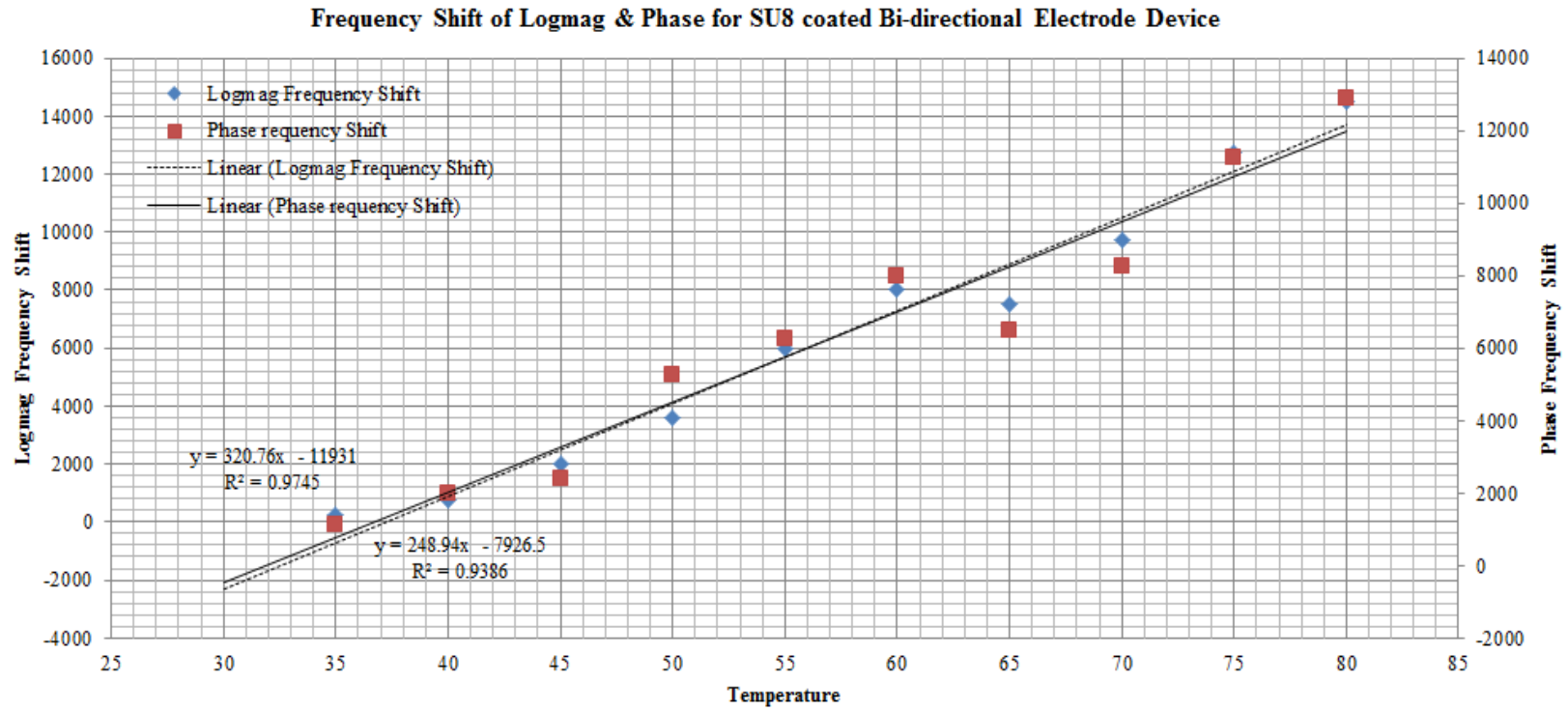


Figure 34 Frequency shift for SU8 coated bi-directional electrode sensor

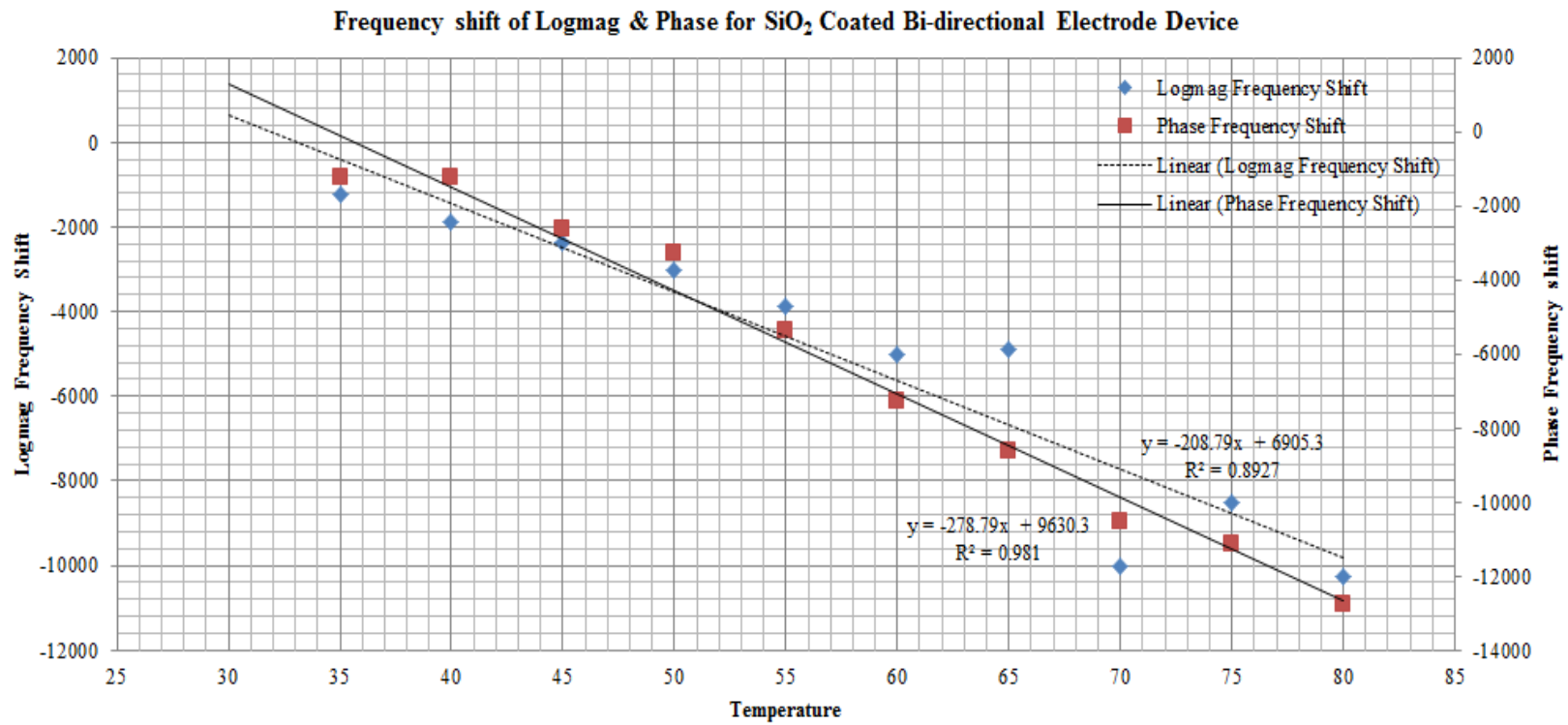


Figure 35 Frequency shift for SiO₂ coated bi-directional electrode sensor

4.2.2 Comparison of Split Electrode Love Wave Sensors

As discussed previously split electrode configuration reduces signal reflection in IDT. Split electrode Love wave sensors should show improved performance with waveguides in their design.

Figure 36 showing SU8 coated split electrode sensor response to temperature. It is observed that, again due to viscoelasticity frequency shift is towards positive. It is also determined that sensor showed very good response to change in temperature for both logarithmic magnitude and phase with ideal linearity in frequency shift.

Figure 37 is plot showing frequency response of SiO₂ coated split electrode sensor. Here phase shift illustrated higher sensitivity and linearity than logarithmic magnitude. Also here frequency shift is negative unlike SU8 Love wave sensors.

On analyzing both SU8 love wave sensor and SiO₂ love wave sensor, it is observed that SU8 coated split electrode sensor comparatively showed three times higher response to temperature than SiO₂ coated split electrode sensor. Also SU8 split electrode Love wave sensor showed better stability and linearity than SiO₂ split electrode Love wave sensor. It is observed from the graphs that phase shift is more responsive to temperature change for both SU8 and SiO₂ split electrode love wave sensors. Also it can be observed that SU8 split electrode sensor showed response in positive direction, which is due to viscoelastic effect in SU8.

Frequency Shift of Logmag & Phase for SU8 Coated Split Electrode Device

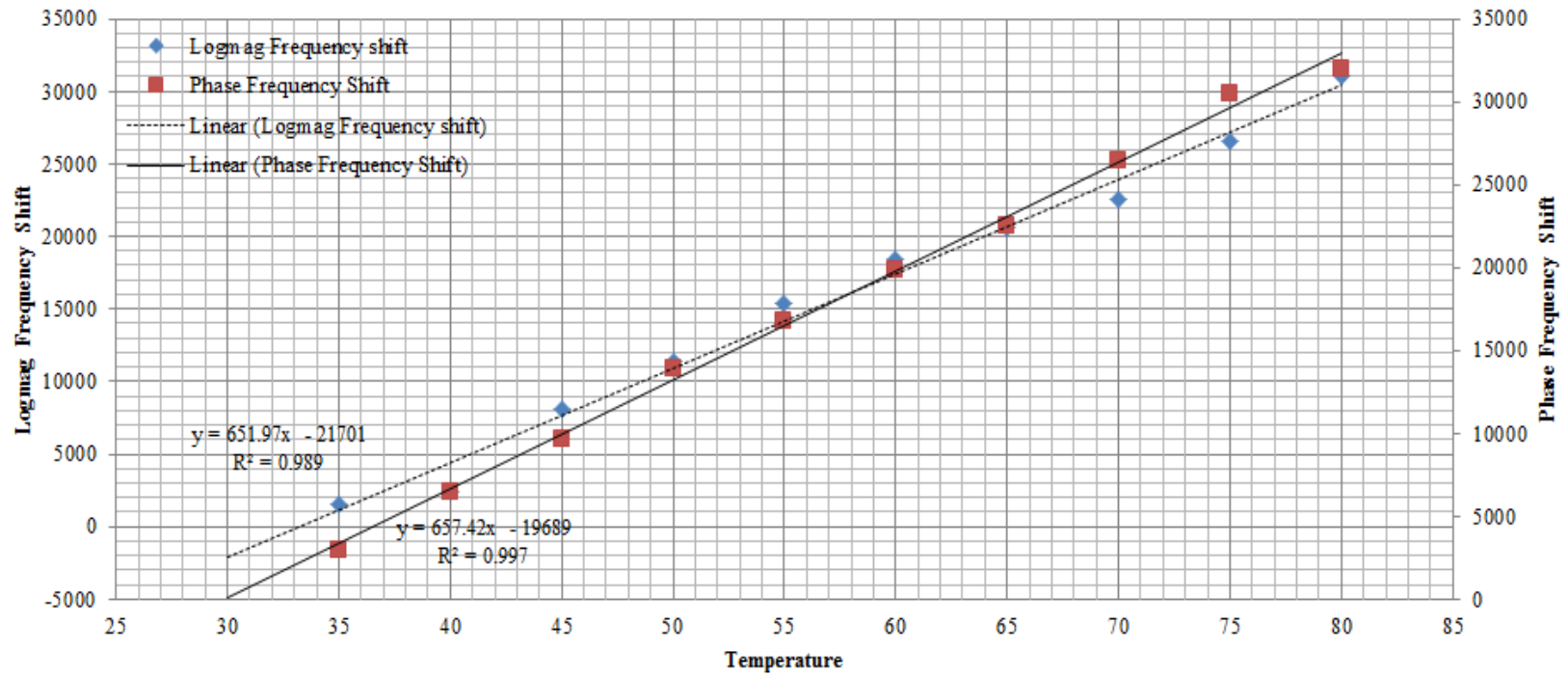


Figure 36 Frequency shift for SU8 coated split electrode sensor

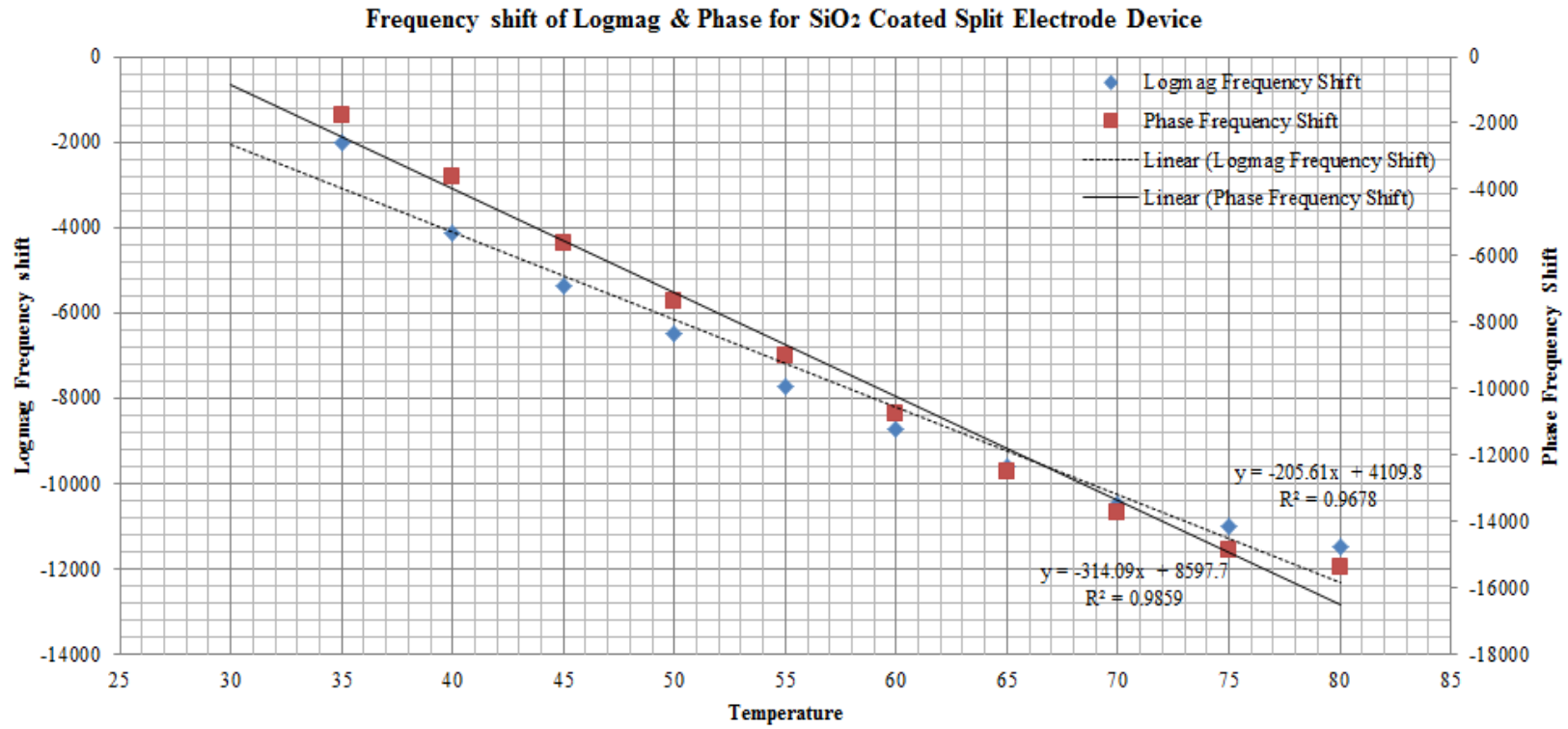


Figure 37 Frequency shift for SiO₂ coated split electrode sensor

4.2.3 Comparison of STW Love Wave Sensors

STW sensors with grating on the delay line tend to be vulnerable to corrosion [71]. With waveguides on STW sensors it can be used in any environment.

Figure 38 shows frequency response of SU8 coated STW sensor. Even though phase and logarithmic magnitude shift followed similar trend, frequency shift for both showed low linearity. Here phase comparatively showed slightly better response to temperature. Also frequency shift was positive due to viscoelastic effect.

Figure 39 shows frequency response for SiO₂ coated STW sensor. Here sensor showed exactly same response and linearity for both logarithmic magnitude and phase with temperature change.

Comparing both sensors, it was determined that SiO₂ coated STW sensor showed better response for both logarithmic magnitude and phase. Also it showed better stability in frequency shift with temperature change. The possible reason for this behavior is due to signal reflection in the metal grating and higher damping of signal with increase in thickness of waveguide material. But it can be observed from the graph that logarithmic magnitude showed higher linearity for both SU8 and SiO₂ STW love wave sensors.

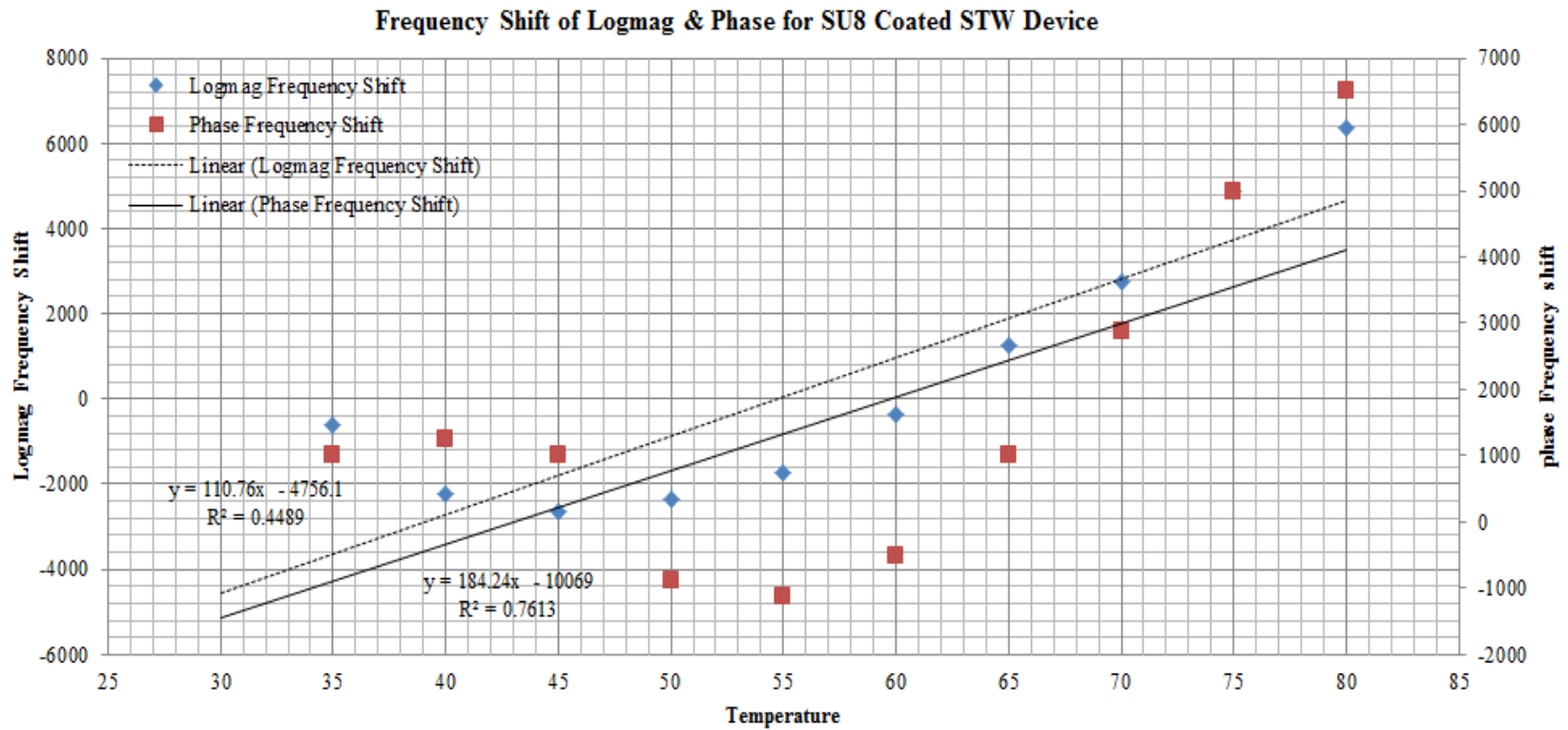


Figure 38 Frequency shift for SU8 coated STW sensor

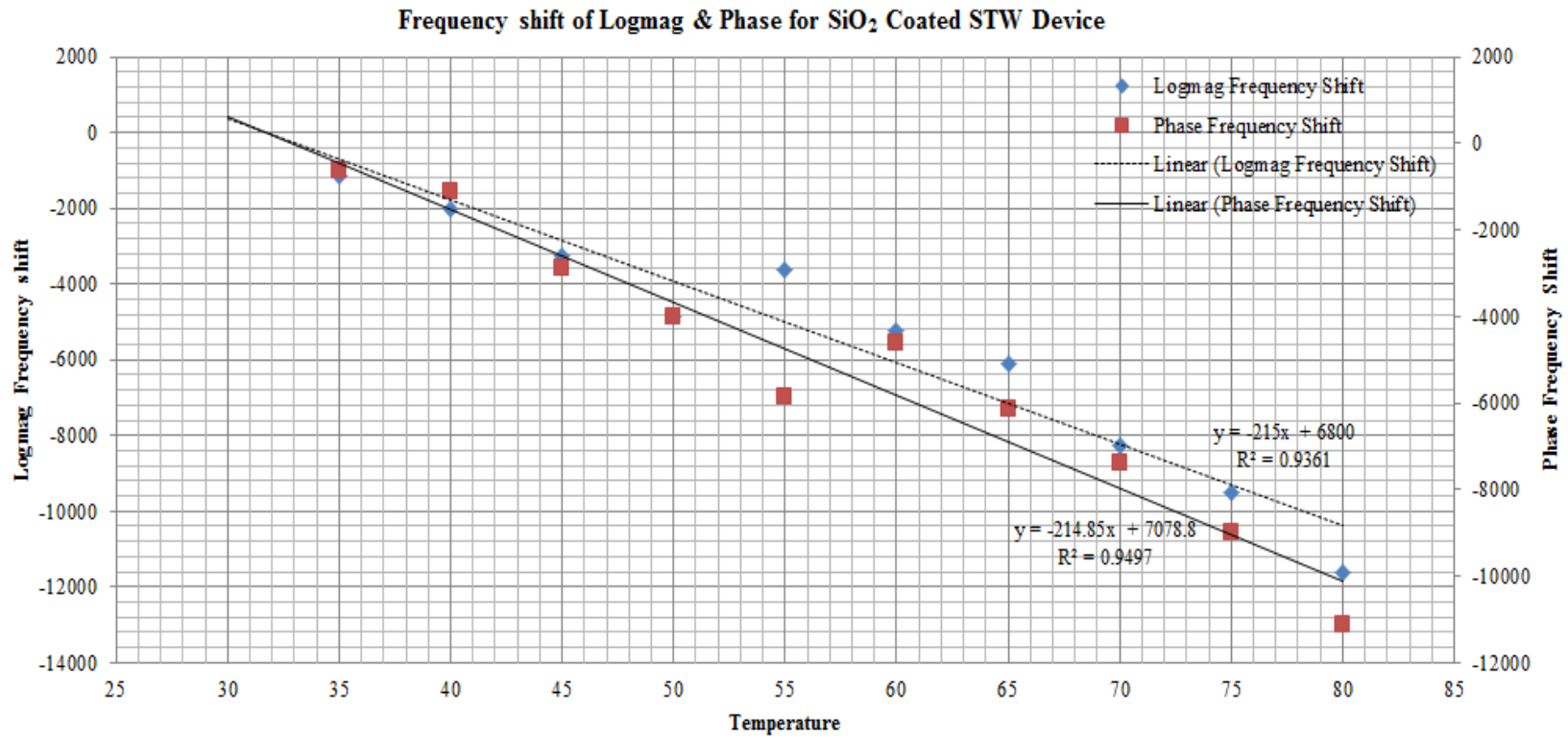


Figure 39 Frequency shift for SiO₂ coated STW sensor

4.2.4 Comparison of SPUDT Love Wave Sensors

SPUDT is reported to reduce signal reflection and improve sensor performance [37]. With wave guide on IDT, improved performance is expected.

Figure 40 illustrated frequency shift of logarithmic magnitude and phase for SU8 coated SPUDT sensor. Logarithmic magnitude showed very high sensitivity to temperature compared to phase shift. Also linearity for both logarithmic magnitude and phase were nearly identical. Again here due to viscoelasticity frequency shift is positive.

Figure 41 shows frequency response of logarithmic magnitude and phase for SiO₂ coated SPUDT sensor. Even though logarithmic magnitude response is slightly higher than phase response, response trend looks exactly same for both. Also both logarithmic magnitude and phase showed same stability and linearity in frequency shift.

When compared it can be observed that SU8 coated SPUDT sensor is very much better than SiO₂ coated SPUDT sensor. SU8 coated SPUDT sensor showed three times better response to temperature for all measurement methods. It also showed good stability and linearity in frequency shift all through the temperature change. It can be observed from the graph that for both SU8 coated SPUDT love wave sensor and SiO₂ coated SPUDT love wave sensor logarithmic magnitude shift showed better sensitivity to temperature change.

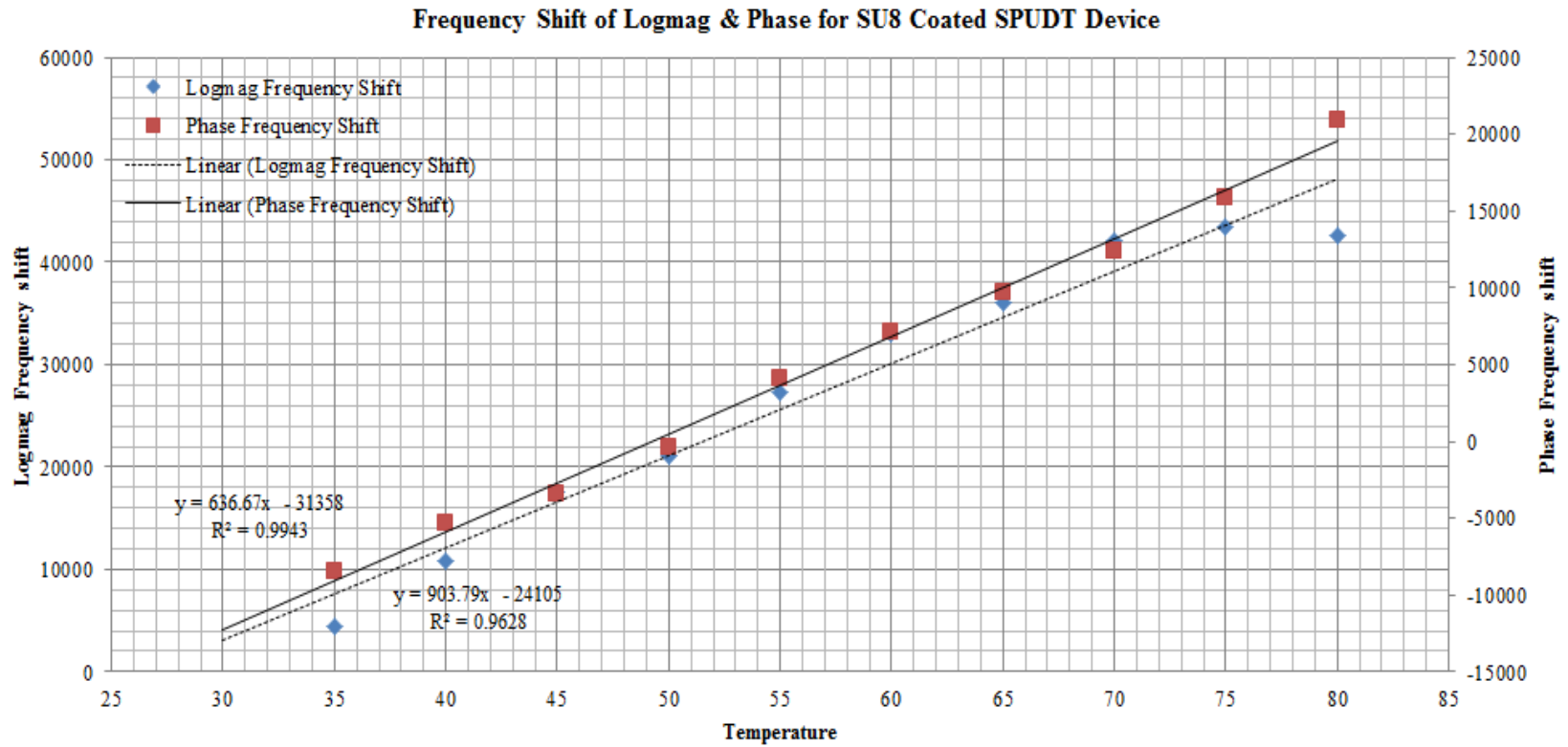


Figure 40 Frequency shift for SU8 coated SPUDT sensor

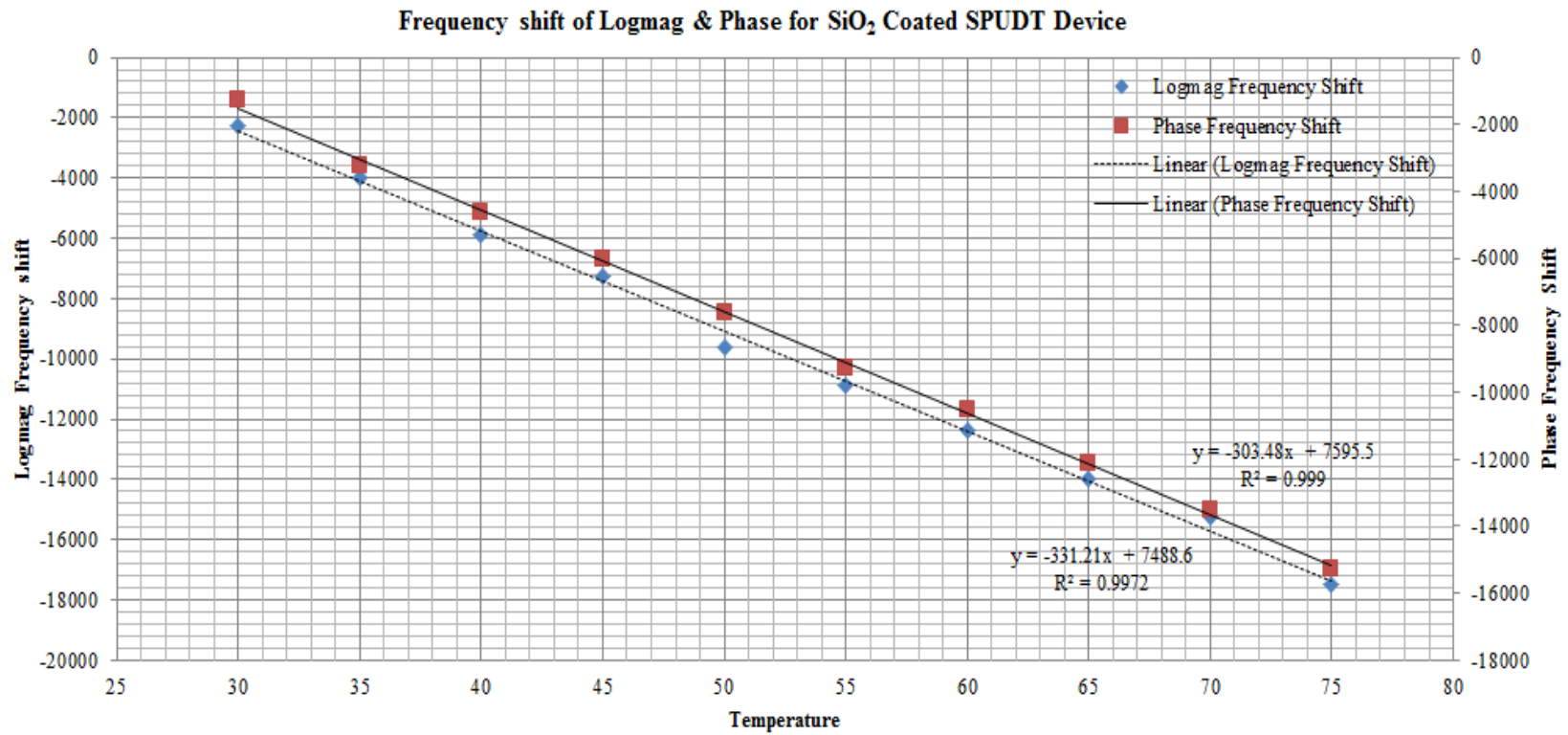


Figure 41 Frequency shift for SiO₂ coated SPUDT sensor

4.2.5 Summary

Table 3 Comparison of SU8 and SiO₂ coated sensors

Sensor/Format		Logarithmic Magnitude		Phase	
		Equation	R ²	Equation	R ²
SU8 Coated	Bi-directional	Y= 248.9x - 7926.5	0.9386	Y= 320.7x - 11931	0.9745
	Split Electrode	Y= 651.9x - 21701	0.9890	Y= 657.4x - 19689	0.9970
	STW	Y= 110.7x - 4756.1	0.4489	Y= 184.2x - 10069	0.7613
	SPUDT	Y= 903.8x - 24105	0.9628	Y= 636.6x - 31358	0.9943
SiO ₂ Coated	Bi-directional	Y= -208.8x+6905.3	0.8927	Y= -278.8x+9630.3	0.9810
	Split Electrode	Y= -205.6x+4109.8	0.9678	Y= -314.1x+8597.7	0.9859
	STW	Y= -215.0x+6800.0	0.9361	Y= -214.8x+7078.8	0.9497
	SPUDT	Y= -331.2x+7488.6	0.9972	Y= -303.4x+7595.5	0.9990

Table 3 here shows all the analyzed data for SU8 and SiO₂ coated sensors. When all SU8 coated sensor are compared, it can be clearly determined that split electrode and SPUDT sensors showed very high sensitivity in both logarithmic magnitude and phase. Also when linearity is observed again clearly split electrode and SPUDT show uniform linearity with increase in temperature.

On comparing sensors with SiO₂ as a waveguide, split electrode here showed better phase response to temperature. SPUDT sensor showed better performance and

optimum linearity than other sensors. It showed good stability in frequency shift all through temperature.

By comparing all SU8 and SiO₂ coated sensors from the table 4.2 it can be inferred that SU8 coated split electrode and SPUDT sensors showed best response to temperature of all. But when linearity is compared SiO₂ coated SPUDT sensors showed highest linearity all through temperature than any sensors above.

5. Conclusion and Future Work

5.1 Conclusion

In this work temperature measurement using surface acoustic wave sensors with different design configurations is presented. Here sensors with different IDT structure and waveguides are designed, fabricated and investigated for sensor response to temperature change.

Sensor response to temperature change is basically investigated by studying phase and logarithmic magnitude shift against temperature. Sensor response is recorded for every $5^{\circ}\text{C}\pm 0.5$ increment starting from 30°C to 80°C . Data recorded in phase and logarithmic magnitude format are analyzed by plotting graph of phase and logarithmic magnitude shift on y-axis and temperature on x-axis.

One objective of this study is to investigate and compare sensors fabricated from wafers sputtered at two different places Nanotechnology Research & Education Center (in-house) and commercial vendor (outside). Here sensors with four different configurations bi-directional, STW, split electrode and SPUDT for both sputtering type were analyzed. By observing results it can be observed that bi-directional electrode configuration showed consistent response and linearity for both sputtering type. When

considered individually in-house sputtered STW, outside sputtered SPUDT and outside sputtered bi-directional electrode configurations showed higher sensitivity and linearity for logarithmic magnitude. Similarly when considered for phase outside sputtered bi-directional electrode configuration, split electrode configuration and SPUDT configuration showed higher sensitivity and linearity to temperature.

Second objective of this study is to investigate sensors performance with SU8 and SiO₂ as a waveguide material. These waveguide are coated onto wafer using two different methods. SU8 which is a negative resist (polymer) is spun on wafer using spin coat method and SiO₂ is coated using PECVD method. Since these two waveguides are two different material they have different acoustic velocity and properties. So their response to surface perturbation will be different from each other.

When these sensors were investigated, it was observed that SU8 waveguide sensors clearly showed very high sensitivity for both logarithmic magnitude and phase compared to SiO₂ waveguide sensors, except for STW sensor configuration. This is due to excessive internal reflection of signal in grating for STW sensors. It was also observed that SU8 Love wave sensors response was contradictory to the SiO₂ Love wave sensors. And the reason for this behavior is viscoelastic effect in SU8 which caused frequency shift in positive direction.

The result from the study showed that improvement in sensitivity, linearity and stability is possible by confining the wave onto the waveguide of the sensor.

5.2 Future Work

Potential future work areas are measuring sensor response in other formats to investigate: insertion loss, response time, and mass loading which gives better information in analyzing sensor performance.

Exclusively designed oscillator circuit can be employed to sensors and investigate sensor response. This will give wider bandwidth for measuring sensor performance.

Current sensor configurations can be applied to measure other different applications, such as humidity, viscosity, pressure, stress, strain and more.

In this study, waveguide is tested for only one thickness. Sensor performance can be investigated for varied waveguide thickness and compared to find the optimum thickness of waveguide that gives highest sensitivity.

Sensors with different waveguide materials can be investigated and compared with current waveguide material.

For this study quartz is the only substrate investigated. Sensor performance with same configuration but for different substrate materials can be investigated and compared.

References

- [1] John Vetelino and Aravind Reghu, *Introduction to Sensors*, CRC Press, Florida, 2011.
- [2] Steven S. Saliterman, *Fundamentals of BioMEMS and Medical Microdevices*, SPIE-The International Society for Optical Engineering, Washington, 2006.
- [3] Jay W. Grate, Stephen J. Martin, Richard M. White, *Acoustic Wave Microsensors Part I*, Analytical Chemistry, Vol. 65, No. 21, 1993.
- [4] Michael J. Vellekoop, *Acoustic Wave Sensors and their Technology*, Ultrasonics, Vol. 36. pp. 7-14, 1998.
- [5] Antonio Arnau *Piezoelectric Transducers and Applications, Second Edition*, Springer, 2010.
- [6] Bill Drafts, *Acoustic Wave Technology Sensors*, IEEE Microwave Theory and Techniques, Vol. 29, No. 4, 2001.
- [7] G.Z. Sauerbrey, *Use of a quartz vibrator for weighing thin layers on a microbalance*, Z. Phys., Issue.55, pp.206-210, 1959.
- [8] C. Andle and J. F. Vetelino, *Acoustic wave biosensors*, IEEE Ultrasonics Symposium, pp.451-460, 1995.
- [9] V.Mecea, *Loaded Vibrating Quartz Sensors*. Sensors & Actuators A 40, pp.1-47, 1994.
- [10] F.Josse, *Acoustic Wave liquid Phase based Microsensors*, Sensors & Actuators, A 44, pp.199-208, 1994.
- [11] Jeffrey Andle, Reichl Haskell and Maly Chap, *Electrically Isolated Thickness Shear Mode Liquid Phase Sensor for High Pressure Environments*, IEEE International Ultrasonics Symposium, pp. 1128-1133, 2008.

- [12] Maria-Isabel Rocha-Gaso, Carmen March-Iborra, Angel Montoya-Baides and Antonio Arnau-Vives, *Surface Generated Acoustic Wave Biosensors for the detection of Pathogens: A Review*, Sensors, Iss.9, pp.5740-5769, 2009.
- [13] Kerem Durdag, *Solid State Acoustic Wave Sensors for Real-time In-line Measurement of Oil Viscosity*, Sensor Review, Emerald, Vol. 28 Iss.1, pp.68 – 73, 2008.
- [14] Rayleigh, J.W.S, *Waves propagated along the plane surface of an elastic solid*, Proceedings of the London Mathematical Society, Vol. 17, No. 1, pp. 4-11, 1885.
- [15] White, R.M. and Voltmer, F.W, *Direct piezoelectric coupling to surface electric waves*, Applied Physics Letters, Vol. 7, pp. 314-316, 1965.
- [16] Marija F. Hribsek, Dejan V. Tomic, Miroslav R. Radosavljevic, *Surface Acoustic Wave Sensors in Mechanical Engineering*, Faculty of Mechanical Engineering, Vol. 38, pp 11-18, 2010.
- [17] Thompson, M. and D.C. Stone, *Surface-Launched Acoustic Wave Sensors: Chemical Sensing and Thin-Film Characterization*. Chemical Analysis, ed. J.D.Winefordner. Vol. 144, New York: John Wiley & Sons, Inc., 1997.
- [18] Julian W. Gardner, Vijay K. Varadan, Osama O. Awadelkarim, *MEMS and Smart Devices*, John Wiley and Sons Ltd, 2007.
- [19] <http://www.exploratorium.edu/faultline/activezone/slides/rlwaves-slide.html> (cited on 09/12/2012).
- [20] He Y. Aoki, Y. Sekimoto, Y. Wada, W. Yamaguchi, R. Nomura, Y. Okuda, *Velocity and damping of the SH-SAW in normal liquid*, Physica B, 329-333, pp.116-117, 2003.
- [21] http://www.wsi.tum.de/Portals/0/Media/Lectures/20082/98f31639-f453-466d-bbc2-a76a95d8dead/BiosensorsBioelectronics_lecture10.pdf (cited on 10/08/2012).
- [22] G.Kovacs, G.W. Lubking, M.J. Vellekoop and A. Venema, *Love wave for (bio)chemical sensing in liquids*, Proc. IEEE Ultrasonics Symp., pp.281-285, 1992.
- [23] J. Du, G.L. Harding, J.A. Ogilvy, P.R. Dencher and M. Lake , *A study of Love-wave acoustic sensors*, Sensors and Actuators A, 56:211-219, 1996.
- [24] http://www.sengenuity.com/tech_ref/AWS_WebVersion.pdf (cited on 10/08/2012).

- [25] Vesseline L. Strashilov and Ventsislav M. Yantchev, *Surface Transverse Waves: Properties, Devices and Analysis*, IEEE Ultrasonics, Ferroelectrics and Frequency Control, Vol. 52, No. 5, 2005.
- [26] R.L. Baer, C.A. Flory, M. Tom-Moy and D.S.-Solomon, *STW Chemical Sensors*, IEEE Ultrasonics Symp., pp0000-0293, 1992.
- [27] Ayca Yurtsever and Ahmed H. Zewail, *Kikuchi ultrafast nanodiffraction in four-dimensional electron microscopy*, PNAS, Vol. 108, No.8, pp.3152-3156, 2011.
- [28] Meirion Lewis, *Surface Skimming Bulk Wave, SSBW*, IEEE Ultrasonics Symp., 1977.
- [29] E. Gavignet, S. Ballandras, E. Bigler, C. Bonjour, J.C. Renaud, *Analysis and experimental study of surface transverse wave resonators on quartz*, J. Appl. Phys. 79, 8944-8950, 1996.
- [30] A. Jhunjhunwala, J.F. Vetelino, D. Harmon and W. Soluch, *Theoretical Examination of Surface Skimming Bulk Waves*, IEEE Ultrasonics Symp., 1978.
- [31] C. K. Campbell, *Surface Acoustic Wave devices for Mobile and Wireless Communication*, Applications of Modern Acoustics, Academic Press Inc., 1998.
- [32] <http://www.aurelienr.com/electronique/piezo/piezo.pdf> (cited on 10/04/2012).
- [33] Colin K. Campbell, *Application of Surface Acoustic and Shallow Bulk Acoustic Wave Devices*, IEEE Proceedings, Vol. 77, No. 10, 1989.
- [34] Kourosh Kalantar-Zadeh, David A. Powell, Wojtek Wlodarski, Samuel Ippolito , Kosmas Galatsis , *Comparison of layered based SAW sensors*, Elsevier Sensors and Actuators, B 91, pp.303-308, 2003.
- [35] James Friend and Leslie Y. Yeo, *Microscale acoustofluidics: Microfluidics driven via acoustics and ultrasonics*, American Physical Society, vol. 83, No.2, pp.647-703, 2011.
- [36] Ballantine, D.S., R.M. White, S.J. Martin, A.J. Ricco, E.T. Zellers, G.C. Frye, and H. Wohltjen, *Acoustic Wave Sensors: Theory, Design, and Physico-chemical Applications*. Applications of Modern Acoustics, San Diego: Academic press. xii, 436, 1997.
- [37] Haekwan Oh, Keekeun Lee, Kyoungtae Eun, Sung-Hoon Choa and Sang Sik Yang, *Development of a high-sensitivity strain measurement system based on a SH SAW sensor*, IOP Publishing Ltd, 2012.
- [38] <http://microchem.com/Tech-LithoTerms.htm> (cited on 09/20/2012)

- [39] Xu Ma and Gonzalo R.Arce, *Computational Lithography*, John Wiley & Sons, Inc. New Jersey, 2010.
- [40] <http://www.azem.com/en/Products/Lithotechnology/Photoresist%20Developers.aspx> (cited on 09/22/2012).
- [41] Stephen D. Senturia, *Microsystem Design*, Kluwer academic publishers, 2001.
- [42] Moussa Hoummady, Andrew Campitelli and Wojtek Wlodarski, *Acoustic wave sensors: design, sensing mechanisms and applications*, IOP Publishing Ltd., pp.647-657, 1997.
- [43] John P.Uyemura, *Physical Design of CMOS integrated Circuits using L-EDIT*, PWS Publication Company, Boston, 2005.
- [44] Campbell, C, *Surface Acoustic Wave Devices and their Signal Processing Applications*, Academic Press, New York, 1998.
- [45] http://www.emsdiasum.com/microscopy/technical/datasheet/sputter_coating.aspx (cited on 10/02/2012).
- [46] http://www.etafilm.com.tw/PVD_Sputtering_Deposition.html (cited on 09/28/2012).
- [47] <http://www.clean.cise.columbia.edu/process/spintheory.pdf> (cited on 09/23/3012).
- [48] David B. Hall, Patrick Underhill & John M. Torkelson, *Spin Coating of Thin and Ultrathin Polymer Films*, Polymer Engineering and Science, December, Vol. 38, No. 12, pp.2039-2045,1998.
- [49] *CZTS (universal element-used In free low-cost CIS based) thin-film solar cell development trend, Part.2*,
<http://www.sneresearch.com/eng/info/show.php?c_id=4970&pg=5&s_sort=&sub_cat=&s_type=&s_word=> (cited on 10/11/2012)
- [50] Mordechai Rothschild, Mark W. Horn, Craig L. Keast, Roderick R. Kunz, Vladimir Liberman, Susan C. Palmateer, Scott P. Doran, Anthony R. Forte, Russell B. Goodman, Jan H.C. Sedlacek, Raymond S. Uttaro, Dan Corliss, and Andrew Grenville, *Photolithography at 193 nm*, The Lincoln Laboratory Journal, Vol. 10, pp.19-34, 1997.
- [51] Kimberly L. Berkowski, Kyle N. Plunkett, Qing Yu and Jeffrey S. Moore, *Introduction to Photolithography: Preparation of Microscale Polymer Silhouettes*, Journal of Chemical Education, Vol. 82 No. 9, pp.1365-1369, 2005.

- [52] Chris A. Mack, *Fundamental Principles of Optical Lithography: The Science of MicroFabrication*, John Wiley & Sons, London, 2007.
- [53] Anssi Hovinen, Alexei Malinin and Antti Lipsanen, *Lithography in Experimental Environment*, Helsinki University of Technology, Electron Physics Laboratory, 2000.
- [54] Darling, E. B. *EE-527: MicroFabrication, Photolithography*. University of Washington, (cited on 09/28/2012).
- [55] Doug Robello, *Quantum Amplification: The Key to Speed*, Lab Rat, Rochester, 2007.
- [56] R. C. Jaeger, *Introduction to Microelectronic Fabrication*, 2nd edition. Auburn, Upper Saddle River - Prentice Hall, 2002.
- [57] M. J. Madou, *Fundamentals of Microfabrication: The Science of Miniaturization*, 2nd edition, CRC Press, 2002.
- [58] K.W. Vogt, M. Houston, M.F. Ceiler, Jr., C.E. Roberts, and P.A. Kohl, *n Dielectric Properties of Low Temperature PECVD Silicon Dioxide by Reaction with Hydrazine*, Journal of Electronic Materials, Vol. 24, No. 6, pp.751-755, 1995.
- [59] PETS, Inc., <http://www.plasmaequip.com/WHAT%20IS%20PECVD.pdf> (cited on 10/07/2012)
- [60] Y. T. Kim, S. M. Cho, Y. G. Seo, H. D. Yoon, Y. M. Im and D. H. Yoon, *Influence of hydrogen on SiO₂ thick film deposited by PECVD and FHD for silica optical waveguide*, WILEY-VCH Verlag GmbH & Co, pp.1257-1263, 2002.
- [61] Thomas Woodson, *Characterization of the Silicon Dioxide Film Growth by Plasma Enhanced Chemical Vapor Deposition (PECVD)*, Princeton Plasma Physics Laboratory, 2004.
- [62] Dr. Jan Verspecht, *Large Signal Network Analysis 'Going beyond S-Parameters*, Jan Verspecht bvba, <http://www.Janverspecht.com> (cited 10/04/2012).
- [63] David Ballo, *Network Analyzer basics*, Hewlett-Packard Company, USA, 1998
- [64] <http://cp.literature.agilent.com/litweb/pdf/5965-7707E.pdf> (cited on 10/06/2012).
- [65] <http://cp.literature.agilent.com/litweb/pdf/5990-5315EN.pdf> (cited on 10/06/2012)

- [66] *Convection oven*, American Heritage Dictionary.
- [67] Operating manual, Quincy Lab Inc., Model GC Series Lab Ovens, Chicago, Illinois, 2008.
- [68] B. Jabby, A. Venema, and M. J. Vellekoop, *Design of Love Wave Sensor Devices for the Operation in Liquid Environments*, IEEE Ultrasonics Symp., 1997.
- [69] Aashish Ahuja, D.L. James, R. Narayan, *Dynamic behavior of ultra-thin polymer films deposited on surface acoustical wave devices*, Sensors and Actuators, 72, pp.234-241, 1999.
- [70] Paul Roach, Shaun Atherton, Nicola Doy, Glen McHale and Michael I. Newton, *SU-8 Guiding Layer for Love Wave Devices*, Sensors,7, pp.2539-2547, 2007.
- [71] Ivan D. Avramov , *Polymer Coated Rayleigh SAW and STW Resonators for Gas Sensor Applications*,Acoustic Waves - From Microdevices to Helioseismology, Intech, 2011.

Appendices

Appendix A: Fabrication Recipes

Table A1 Design parameters

Crystal	ST-Quartz
Acoustic Velocity	5050m/s
Capacitance/unit length, C_0	0.5 pF/cm
Coupling Co-Efficient, K^2	1.9%
Design Impudence, Z	50 Ω
Centre Frequency, f_0	17MHz
Wave Length, λ	300 μ m
Length of transducer, 50λ	6mm
Number of Finger Pairs, N	20
Aperture width, W	6.25mm
Delay Path Length, 100λ	12mm
Bi-Directional Type Fingers	
Width of Finger Pair, $\lambda/4$	75 μ m
Inter digital spacing center to center, $\lambda/2$	150 μ m
Split Electrode	
Width of Finger Pair, $\lambda/8$	37.5 μ m
Inter digital spacing center to center, $\lambda/4$	75 μ m
Single Phase Unidirectional Transducer	
Width of Finger Pair, $\lambda/8$	37.5 μ m
Width of Finger Pair, $\lambda/4$	75 μ m
Gap b/w adjacent fingers, $\lambda/8$	37.5 μ m
Gap b/w adjacent fingers, $3\lambda/16$	56.25 μ m
Guiding Layer	
SiO₂	6 μ m
SU8-2035	40 μ m

Appendix A (Continued)

Table A2 Sputtering condition

Target	Chrome
Wafer	ST-Quartz
Thickness	1000°A
Vacuum	0.01mTorr
Power	200Watt
Time	5minutes

Table A3 Recipe for spin coating

Resist	S1813	SU8 2035
Thickness	1.3µm	40µm
Wafer Preparation	<ul style="list-style-type: none"> • 10min ultrasonic cleaning • Acetone, Methanol, DI water wash and Nitrogen drying 	Acetone, Methanol, DI water wash and Nitrogen drying
Spin Coating	<ul style="list-style-type: none"> • 500rpm for 10seconds for spreading • 3000rpm for 40seconds 	<ul style="list-style-type: none"> • 500rpm for 10seconds for spreading • 3100rpm for 50seconds
Soft Bake	1minute at 90-100°C	<ul style="list-style-type: none"> • 65°C for 3minutes • 95°C for 6minutes
Exposure	Intensity of 25mW/cm ² for 5sec	Intensity of 25mW/cm ² for 6.4sec (Power of 160mJ/cm ²)
Development	AZ726 or MF319 for 70sec	SU8 developer for 5minutes
Hard Bake	5minutes at 100-115°C	10minutes at 150°C
Etching	Chrome etchant	-----

Appendix A (Continued)

Table A4 PECVD recipe for growing SiO₂



Process	Surface Pre-Cleaning	Deposition
Crystal	ST-Quartz	ST-Quartz
Thickness	-----	6μm
RF Power	50 watts, 13.56MHz	50 watts, 13.56MHz
Pressure	800 mTorr	800 mTorr
Chuck Temperature	250°C	250°C
Chamber Temperature	60°C	60°C
N2O Flow	500 sccm	500 sccm
SiH4 Flow	-----	11 sccm
Time	180 sec	10600 sec

Table A5 Dicing saw recipe

Crystal	ST-Quartz
Blade Type	Hubless Diamond Tip blade
Pass 1	29mm
Pass 2	25mm
Height	0.312mm
Depth of Cut	0.81mm
Table turning Angle	90°
Wafer Diameter	89mm
Speed of Cut	20,000rpm (6.3 in instrument)


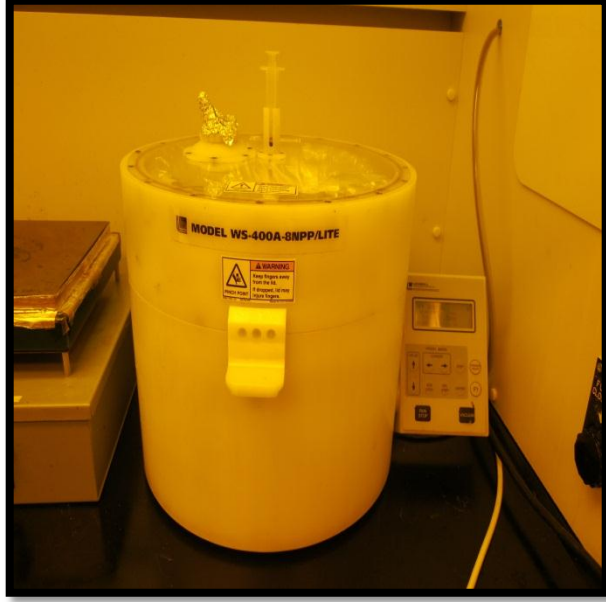
Appendix B: Instrumentation

Table B1 Instruments used for this study

Instrument	Model	Picture
Ultrasonic Cleaner	Branson 1510	
Sputter Coater	CRS-100 Sputtering System	

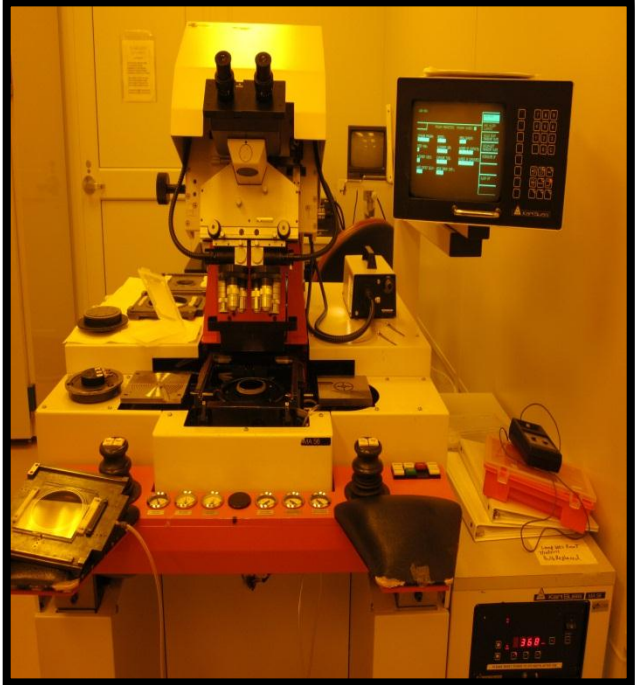

Appendix B (Continued)

Table B1 (Continued)

<p>Alpha-step Profilometer</p>	<p>Brumley South Inc., Model Alpha-step 200</p>	 A photograph of an Alpha-step Profilometer. The device is a light-colored, boxy machine with a small CRT monitor on top. Below the monitor is a control panel with a numeric keypad and several function buttons. The machine is sitting on a white surface in a laboratory setting.
<p>Spin Coating System</p>	<p>Laurel Spinner, Model-WS- 400A- 8NPP/LITE</p>	 A photograph of a Laurel Spinner, Model-WS-400A-8NPP/LITE. It is a large, cylindrical, light-colored container with a central spindle and a motor assembly on top. A warning label is visible on the side of the container. The device is placed on a dark surface next to a control panel.



Appendix B (Continued)

Table B1 (Continued)

<p>Mask Aligner</p>	<p>Karl Suss, Model MA 56</p>	
<p>Compound Microscope</p>	<p>Mitutoyo, Ultraplan, Model FS110</p>	



Appendix B (Continued)

Table B1 (Continued)

<p>Dicing Saw</p>	<p>Micro-Automation, Inc. Dicing SAW Model 1006</p>	 A photograph of a Micro-Automation, Inc. Dicing SAW Model 1006. The machine is a large, industrial-grade dicing saw with a prominent vertical blade assembly. It features a control panel with numerous buttons and a small monitor. The machine is mounted on a sturdy base and is positioned in a laboratory or industrial setting.
<p>Network Analyzer</p>	<p>Agilent Technologies, Model E5061A</p>	 A photograph of an Agilent Technologies E5061A Network Analyzer. The device is a rack-mountable instrument with a large color display screen on the left side. The right side of the front panel is densely packed with various control elements, including a numeric keypad, function keys, and a central rotary knob. Two cables are plugged into the front panel connectors.

Appendix B (Continued)

Table B1 (Continued)

<p>Digital Multi-meter</p>	<p>Agilent Technologies, Model 34405</p>	 A photograph of an Agilent 34405A 5 1/2 Digit Multimeter. The device is a light grey benchtop unit with a large black LCD screen in the center. Below the screen is a control panel with various buttons for functions like Power, DCV, ACV, D, Freq, Auto, Hold, Min/Max, Color, and Temp. To the right of the screen are several input ports, including a 12A port and a 500V port, with red and black test leads plugged into them. The Agilent logo and model number are visible on the top left of the front panel.
<p>Convection Oven</p>	<p>Quincy Lab, Model 20GC Lab Oven</p>	 A photograph of a Quincy Lab Model 20GC Lab Oven. It is a tall, rectangular, light grey convection oven with a black handle on the left side. The front panel features a control knob on the left, a red indicator light labeled "HEAT CYCLE" in the center, and a power switch on the right. The Quincy Lab logo is visible on the bottom left of the front panel. The oven is sitting on a white lab bench.

Appendix C: Copyright Permissions

C.1 Permission for Figure 2, Figure 3, Figure 4 (a) and Figure 5

Permission type selected: Republish or display content

Type of use selected: reuse in a thesis/dissertation

✕✕ [Select different permission](#)

Article title: Acoustic wave technology sensors

Author(s): Drafts, B.


DOI: 10.1109/22.915466

Date: Apr 1, 2001

Volume: 49

Issue: 4 2

✕✕ [Select different article](#)

 [Terms and conditions apply to this permission type](#)
[View details](#)

Thesis / Dissertation Reuse

The IEEE does not require individuals working on a thesis to obtain a formal reuse license, however, you may print out this statement to be used as a permission grant:

Requirements to be followed when using any portion (e.g., figure, graph, table, or textual material) of an IEEE copyrighted paper in a thesis:

- 1) In the case of textual material (e.g., using short quotes or referring to the work within these papers) users must give full credit to the original source (author, paper, publication) followed by the IEEE copyright line © 2011 IEEE.
- 2) In the case of illustrations or tabular material, we require that the copyright line © [Year of original publication] IEEE appear prominently with each reprinted figure and/or table.
- 3) If a substantial portion of the original paper is to be used, and if you are not the senior author, also obtain the senior author's approval.

Requirements to be followed when using an entire IEEE copyrighted paper in a thesis:

- 1) The following IEEE copyright/ credit notice should be placed prominently in the references: © [year of original publication] IEEE. Reprinted, with permission, from [author names, paper title, IEEE publication title, and month/year of publication]
- 2) Only the accepted version of an IEEE copyrighted paper can be used when posting the paper or your thesis on-line.
- 3) In placing the thesis on the author's university website, please display the following message in a prominent place on the website: In reference to IEEE copyrighted material which is used with permission in this thesis, the IEEE does not endorse any of [university/educational entity's name]

Appendix C (Continued)

C.2 Permission for Table 1

Permission type selected: Republish or display content

Type of use selected: reuse in a thesis/dissertation

✖ Select different permission

Article title: Applications of surface acoustic and shallow bulk acoustic wave devices

Author(s): Campbell, C.K.


DOI: 10.1109/5.40664

Date: Oct 1, 1989

Volume: 77

Issue: 10

✖ Select different article

 Terms and conditions apply to this permission type
[View details](#)

Thesis / Dissertation Reuse

The IEEE does not require individuals working on a thesis to obtain a formal reuse license, however, you may print out this statement to be used as a permission grant:

Requirements to be followed when using any portion (e.g., figure, graph, table, or textual material) of an IEEE copyrighted paper in a thesis:

- 1) In the case of textual material (e.g., using short quotes or referring to the work within these papers) users must give full credit to the original source (author, paper, publication) followed by the IEEE copyright line © 2011 IEEE.
- 2) In the case of illustrations or tabular material, we require that the copyright line © [Year of original publication] IEEE appear prominently with each reprinted figure and/or table.
- 3) If a substantial portion of the original paper is to be used, and if you are not the senior author, also obtain the senior author's approval.

Requirements to be followed when using an entire IEEE copyrighted paper in a thesis:

- 1) The following IEEE copyright/ credit notice should be placed prominently in the references: © [year of original publication] IEEE. Reprinted, with permission, from [author names, paper title, IEEE publication title, and month/year of publication]
- 2) Only the accepted version of an IEEE copyrighted paper can be used when posting the paper or your thesis on-line.
- 3) In placing the thesis on the author's university website, please display the following message in a

Appendix C (Continued)

C.3 Permission for Figure 12, Figure 13 and Figure 14

Permission request form

11/05/2012

To whom it may concern

I am preparing a work entitled

"Investigation of Various Surface Acoustic Wave Design Configurations for Improved Sensitivity" to be reused in Thesis (Educational Purpose) by IOP Publishing Ltd which trades as IOP Publishing of Temple Circus, Temple Way, Bristol BS1 6HG, UK.

I would appreciate permission to reproduce the following items in both print and electronic editions of the Journal and in all subsequent future editions of the Journal, any derivative products and in publisher authorized distribution by third party distributors, aggregators and other licensees such as abstracting and indexing services. I should be grateful for nonexclusive perpetual world rights in all languages and media. Unless you indicate otherwise, I will use the complete reference given below as the credit line.

In case you do not control these rights, I would appreciate it if you could let me know to whom I should apply for permissions.

- ✓ 1. **Figure 2 of "Development of a high-sensitivity strain measurement system based on a SH SAW sensor", J. Micromech. Microeng. 22 (2012) 025002 (10pp).**

For material being published electronically a link to the version of record will be provided back to the original article via DOI.

For your information, Institute of Physics Publishing is a not-for-profit subsidiary of the UK Institute of Physics and is a signatory to the STM guidelines on use and republication of figures/tables in science publishing.

For your convenience a copy of this letter may serve as a release form: the duplicate copy may be retained for your files.

Thank you for your prompt attention to this request. Permission is being requested of the authors and the publisher separately.

Yours sincerely

(Greeshma Manohar)

I/We grant permission for the use of the work as set out above.

Signed:

Date:

On behalf of Publisher:

Appendix C (Continued)

PERMISSION TO REPRODUCE AS REQUESTED IS GIVEN PROVIDED THAT:

- (a) the consent of the author(s) is obtained
- (b) the source of the material including author, title of article, title of journal, volume number, issue number (if relevant), page range (or first page if this is the only information available), date and publisher is acknowledged.
- (c) for material being published electronically, a link back to the original article should be provided (via DOI).



IOP Publishing Ltd
Temple Circus
Temple Way
BRISTOL
BS1 6BE

06.11.2012
Date

Sarah Pyle
Rights & Permissions

Appendix C (Continued)

C.4 Permission for Figure 9 (b)

PNAS Permissions Editor
500 Fifth Street, NW
NAS 340
Washington, DC 20001 USA
Phone  202-334-2679 

Anyone may, without requesting permission, use original figures or tables published in PNAS for noncommercial and educational use (i.e., in a review article, in a book that is not for sale) provided that the original source and the applicable copyright notice are cited.

C.5 Permission for Figure 11, Figure 15 and Figure 20



John Wiley & Sons, Ltd

The following material does not generally require permission:

Excerpts falling within the STM Guidelines for Quotation and Other Academic Uses of Excerpts from Journal Articles. You may use the following without obtaining explicit permission from the STM publishers who are signatories to these guidelines: